



BENT CRYSTALS FOR BEAM STEERING IN ACCELERATORS

I.V. Kyryllin

- *NSC Kharkiv Institute of Physics and Technology, Kharkiv, Ukraine*
- *V. N. Karazin Kharkiv National University, Kharkiv, Ukraine*

January 22, 2025

KINR Annual Workshop “High Energy Physics. Theoretical and Experimental Challenges”

Academician of the National Academy of Sciences of Ukraine

Prof. Mykola Shul'ga

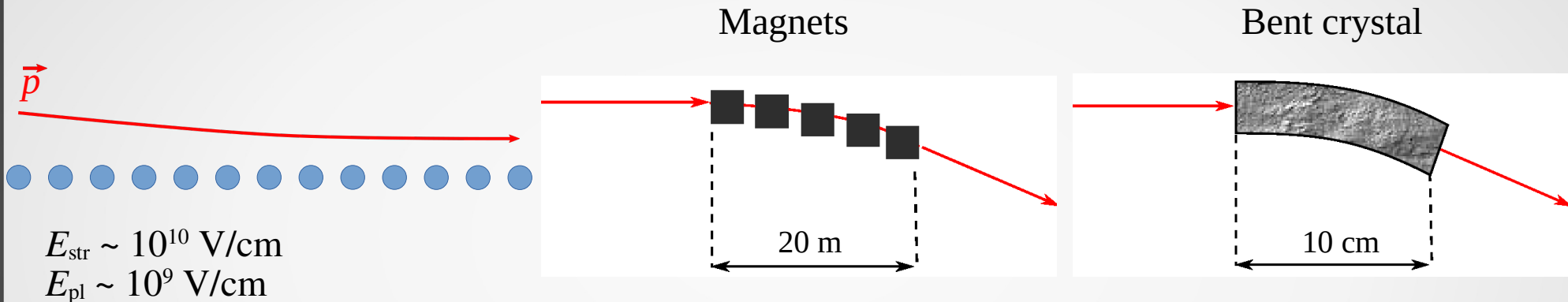


З 1996 р. Микола Федорович Шульга (15.09.1947–23.01.2024) очолював ІТФ ім. О.І. Ахізера

З 2015 р. по 2024 р. Академік-секретар Відділення ядерної фізики та енергетики НАН України

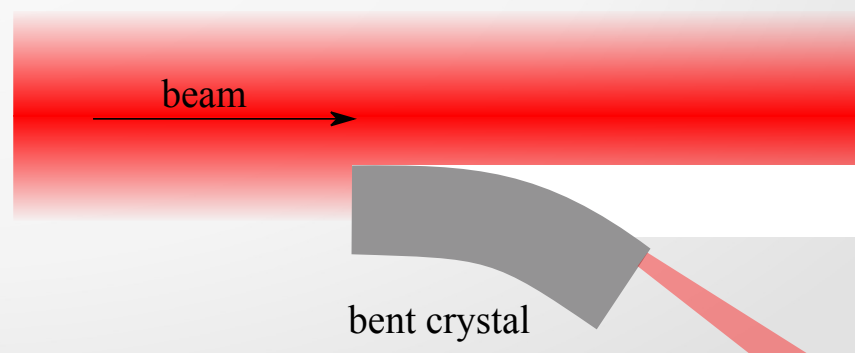
З 2016 р. по 2024 р. Генеральний директор, Національний науковий центр «Харківський фізико-технічний інститут»

Bent crystals and magnetic deflection systems



Advantages of bent crystals in comparison with magnetic deflection systems:

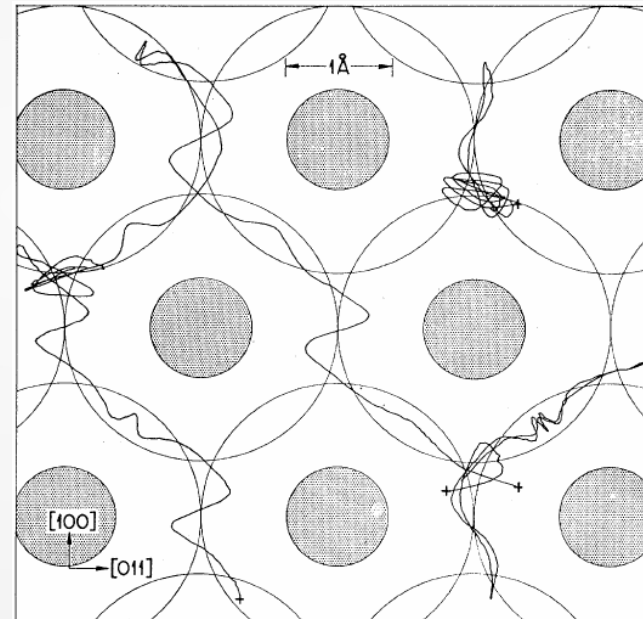
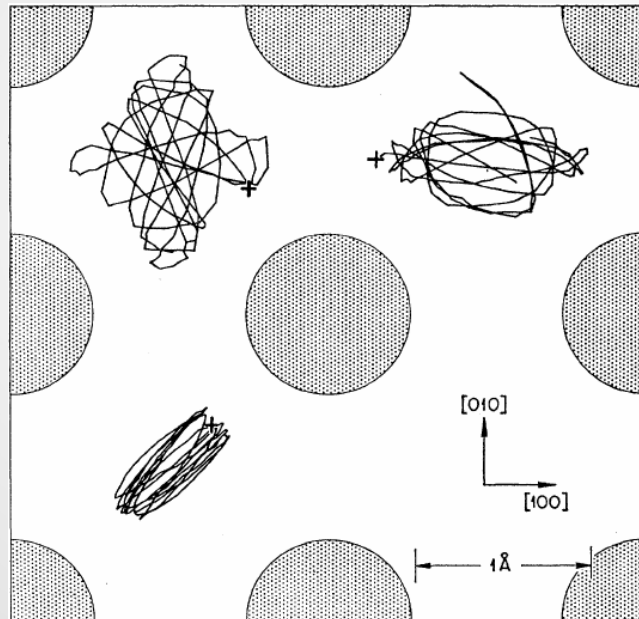
- Small size
- do not need electricity consumption
- do not need cooling



Розсіювання заряджених частинок у кристалі

Robinson M. T., Oen O. S., Holmes D. K. Computer studies of anomalous penetration of Cu recoil atoms in Cu crystal. Proc. of Conference «Bombardment Ionique». CNRS. Paris. 1962. P. 105.

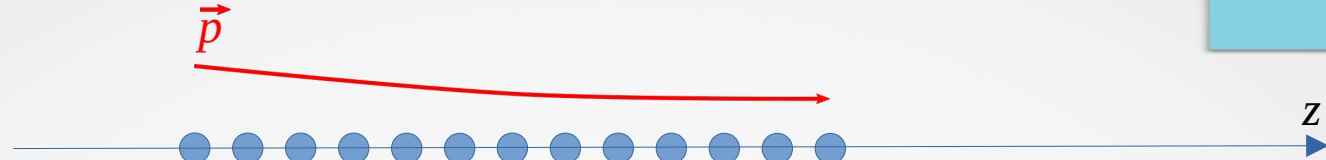
Robinson M. T., Oen O. S. Computer studies of the slowing down of energetic atoms in crystals. Phys. Rev. 1963. Vol. 132, No. 6. P. 2385.



Cu^+ , $E=1\text{-}10 \text{ кэВ}$

Lindhard J. Influence of crystal lattice on motion of energetic charged particles. Mat. Fys. Medd. Dan. Vid. Selsk. 1965. Vol. 34, No. 14. P. 1–64.

Наближення безперервного потенціалу



$$\frac{d}{dt} \frac{m v}{\sqrt{1 - v^2/c^2}} = -q \nabla \Phi_c(\mathbf{r})$$

$$\Phi_c(\mathbf{r}) = \sum_n \Phi_a(\mathbf{r} - \mathbf{r}_n)$$

$$\Phi(\rho) = \frac{1}{L} \int_{-\infty}^{\infty} dz \Phi_c(\rho, z)$$

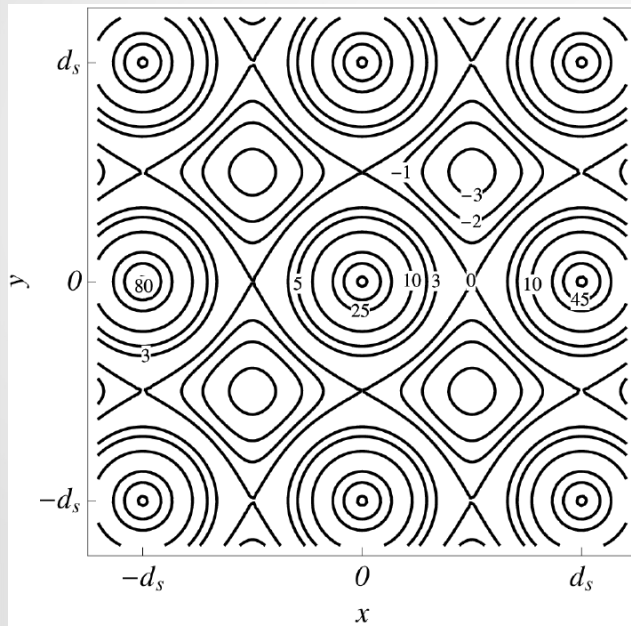
$$\ddot{\rho} = -\frac{c^2 q}{E_{||}} \frac{\partial}{\partial \rho} \Phi(\rho)$$

$$E_{||} = c \sqrt{p_{||}^2 + (mc)^2}$$

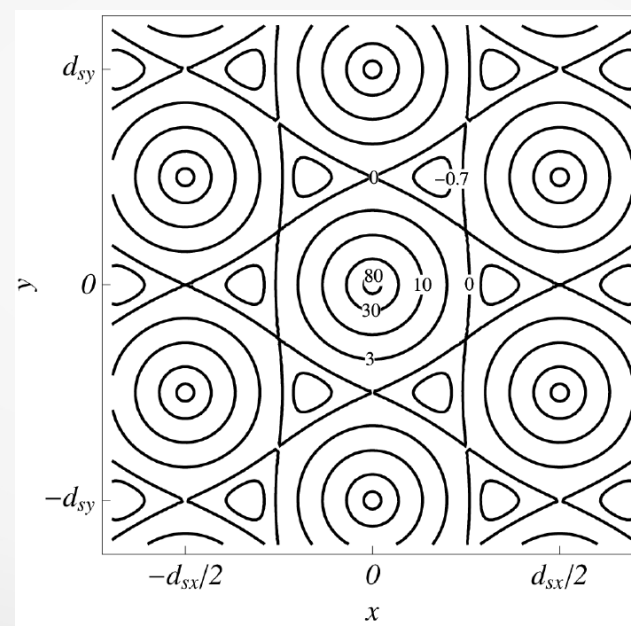
Lindhard J. Influence of crystal lattice on motion of energetic charged particles. Mat. Fys. Medd. Dan. Vid. Selsk. 1965. Vol. 34, No. 14. P. 1–64.

Potential of crystal atomic strings

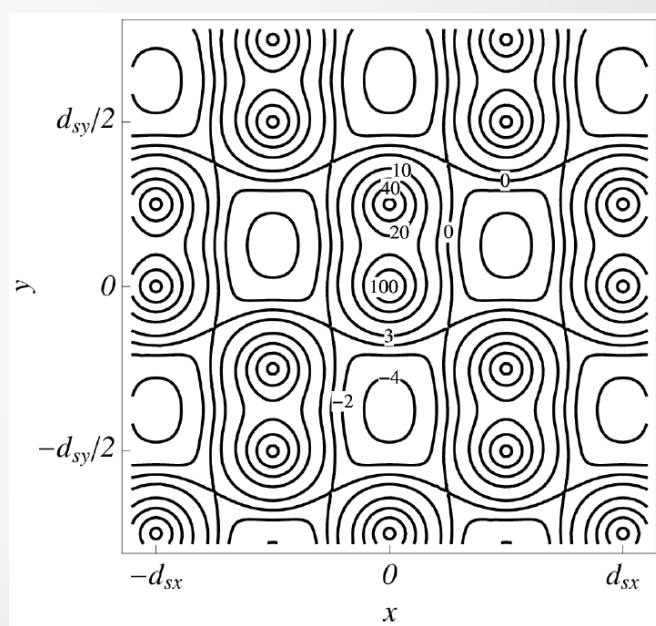
Si <100>



Si <111>

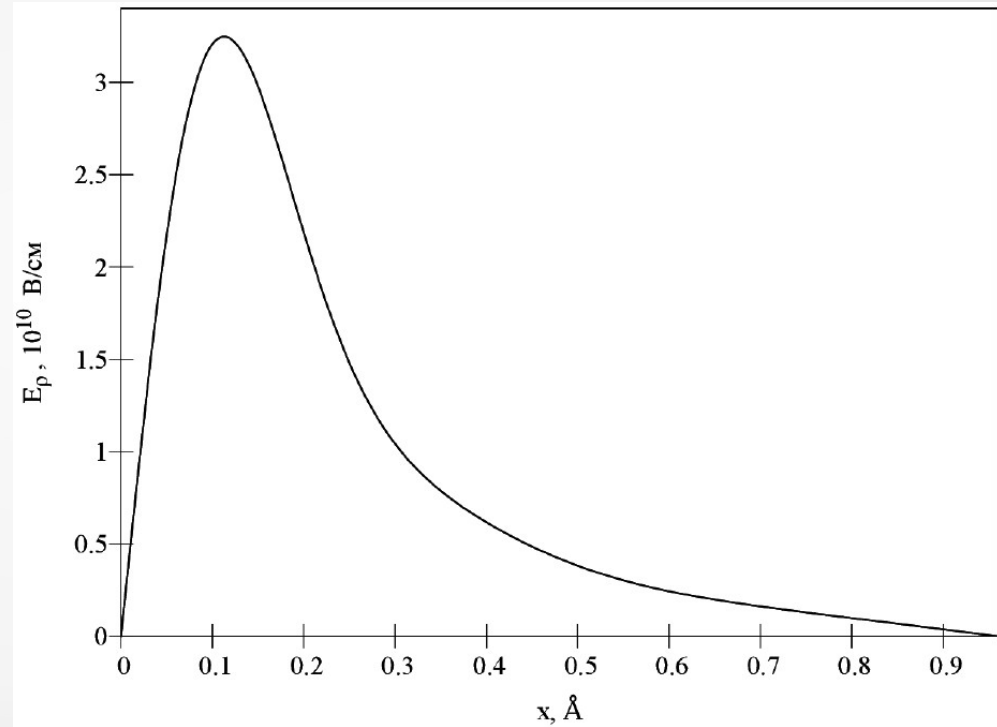
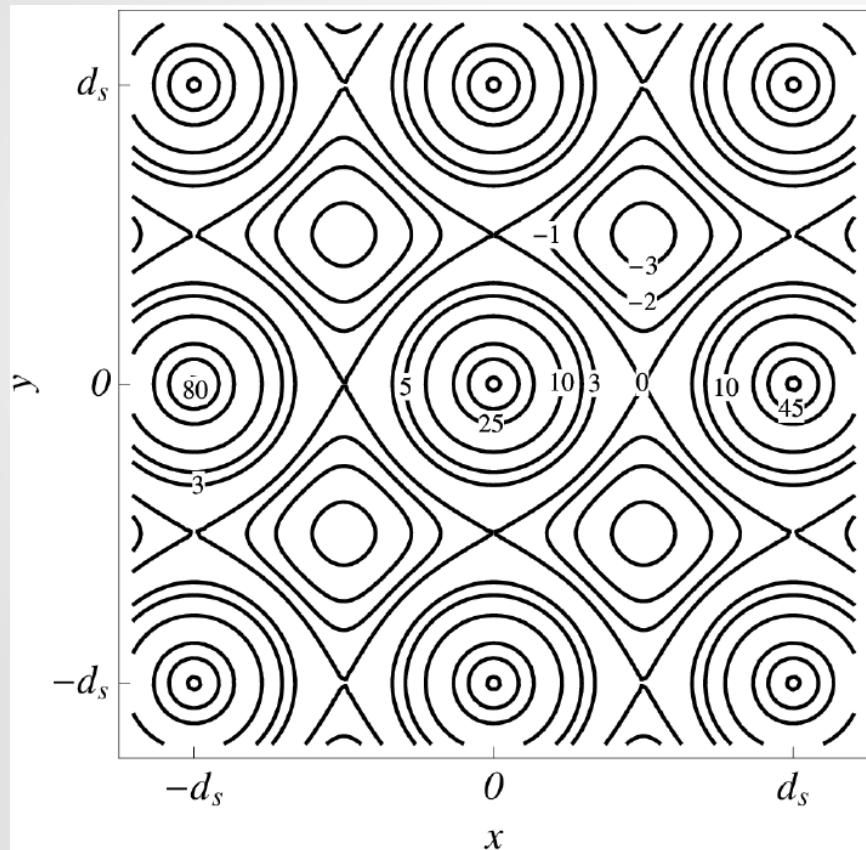


Si <110>



Potential of crystal atomic strings

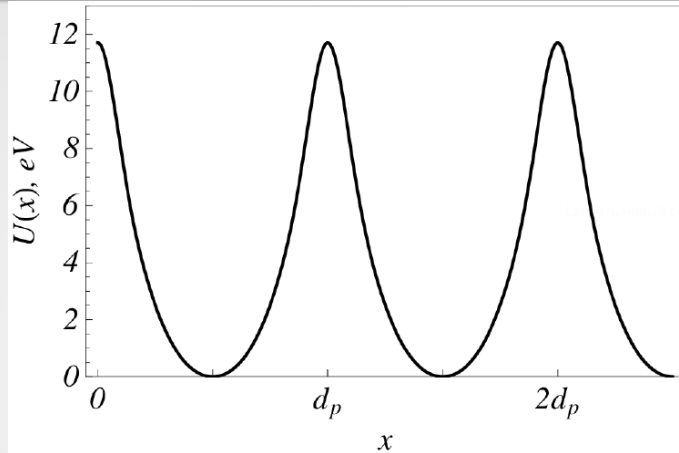
Si <100>



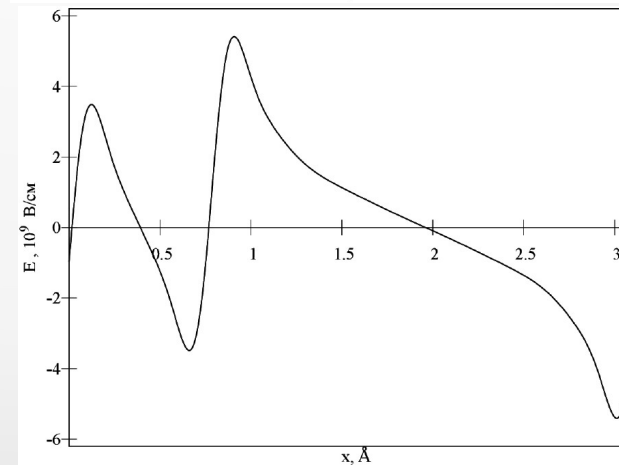
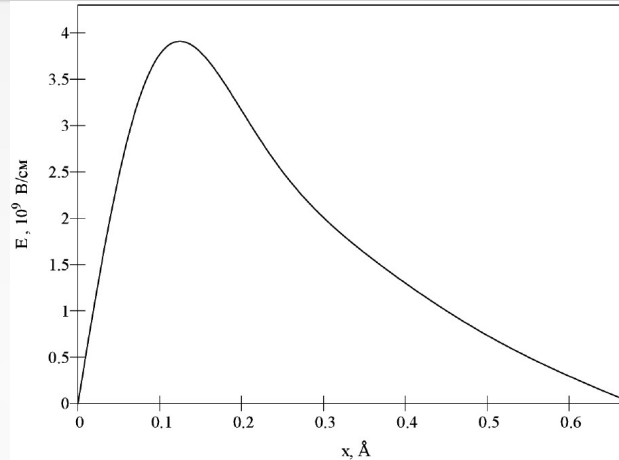
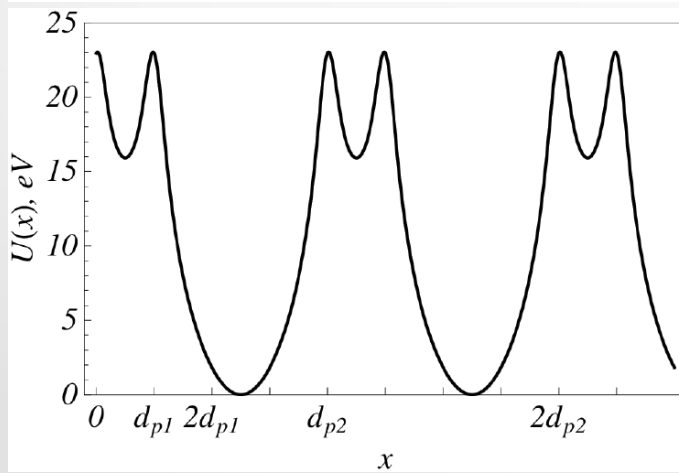
$$E_{\text{str}} \sim 10^{10} \text{ V/cm}$$

Potential of crystal atomic planes

Si (100)



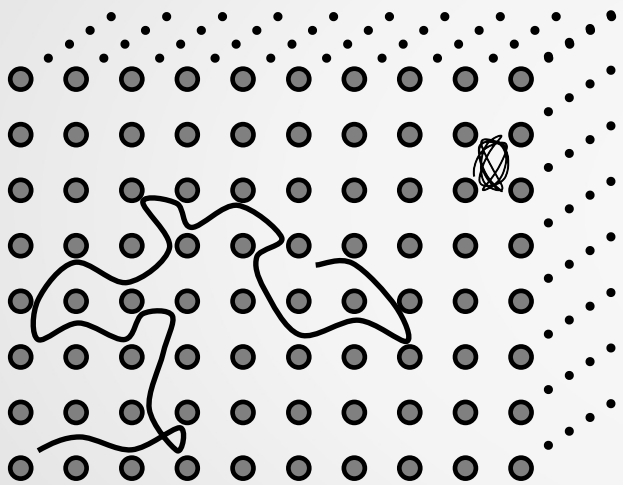
Si (110)



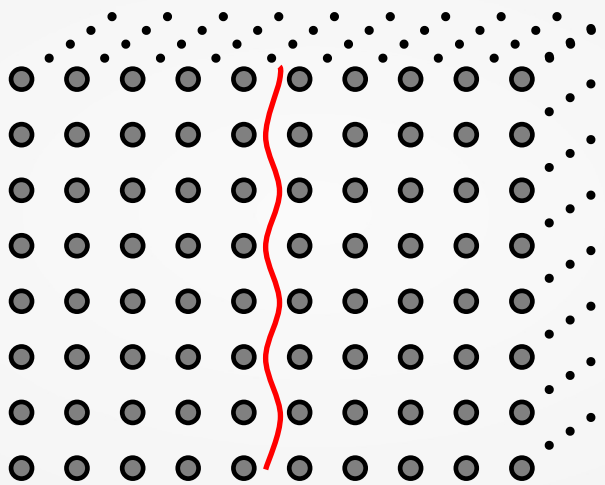
$$E_{\text{str}} \sim 10^{10} \text{ V/cm}$$
$$E_{\text{pl}} \sim 10^9 \text{ V/cm}$$

Regimes of motion in a crystal

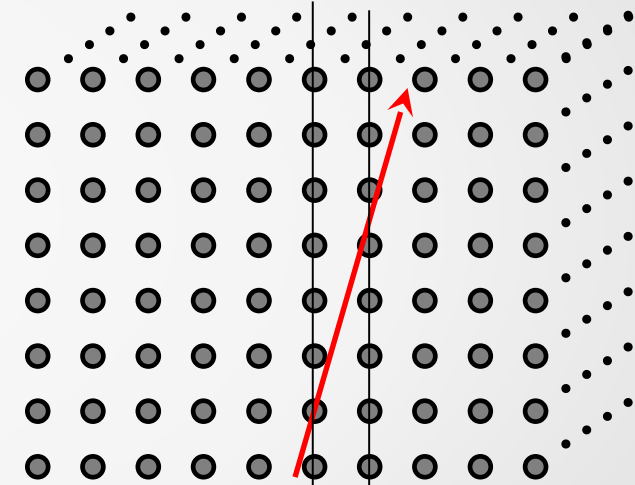
$$\psi_x \approx \psi_y < \psi_c$$



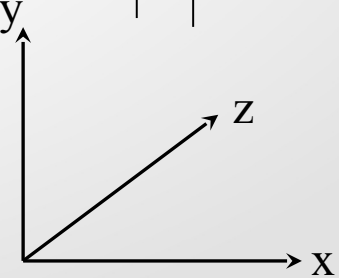
$$\psi_x < \theta_c, \psi_y \gg \psi_c$$



$$\psi_x > \theta_c, \psi_y \gg \psi_c$$

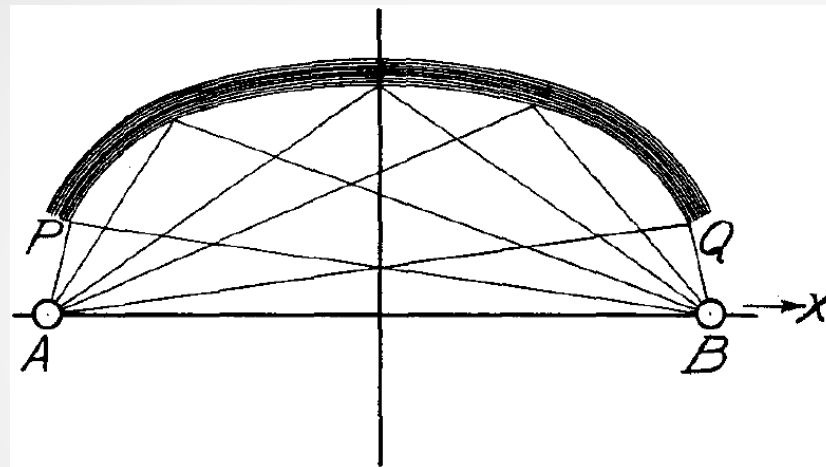


$$v_z \approx c, \quad \psi_x = \frac{v_x}{c}, \quad \psi_y = \frac{v_y}{c}, \quad \psi_c \approx 2\theta_c \sim 10^{-5}$$



Вигнуті кристали в рентгенівській спектроскопії

DuMond J. W., Kirkpatrick H. A. *The multiple crystal x-ray spectrograph*. Rev. Sci. Instrum. 1930. Vol. 1, No. 2. P. 88–105



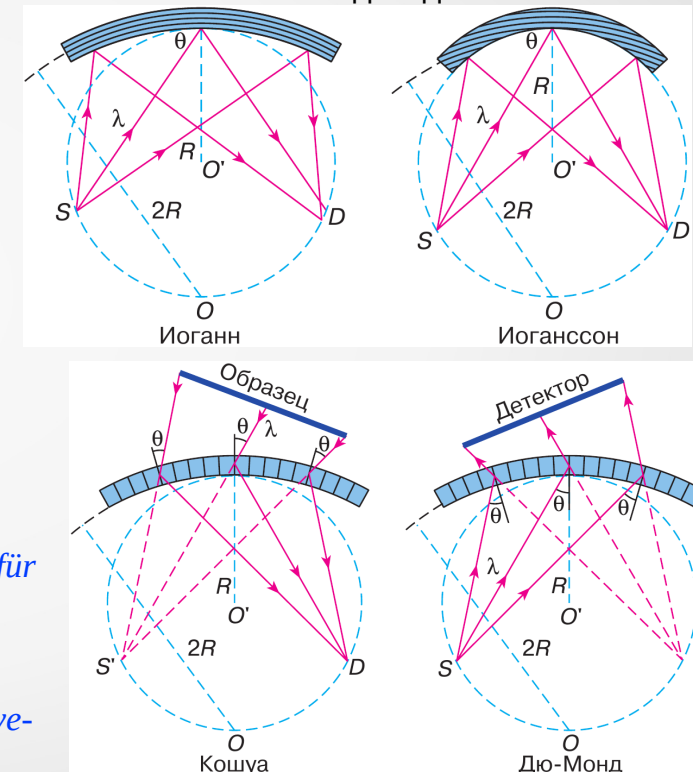
Johann H. *The production-aperture X-ray spectra with the help of concave crystals*. Eur. Phys. J. A. 1931. Vol. 69. P. 185.

Johansson T. *Über ein neuartiges, genau fokussierendes röntgenspektrometer*. Zeitschrift für Physik. 1933. Vol. 82, No. 7-8. P. 507–528.

Cauchois Y. *Spectrographie des rayons X par transmission d'un faisceau non canalisé à travers un cristal courbé (I)*. J. phys. Radium. 1932. Vol. 3, No. 7. P. 320–336.

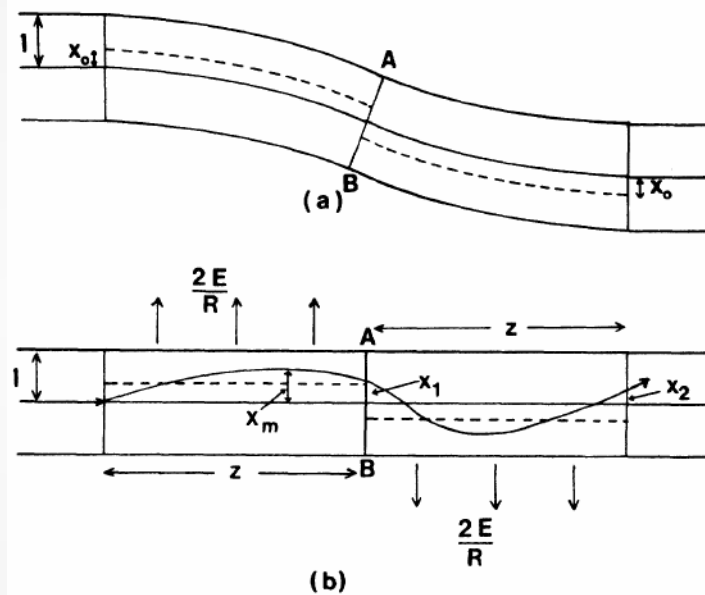
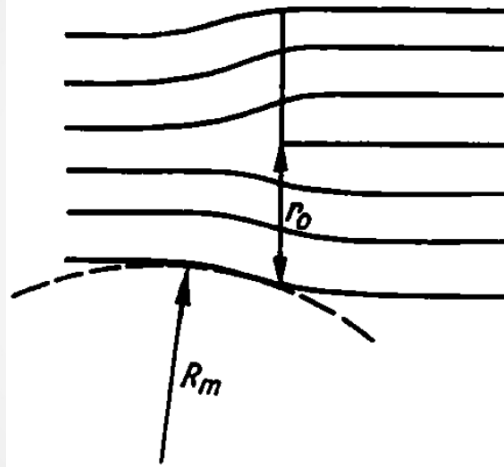
DuMond J. W. *A high resolving power, curved-crystal focusing spectrometer for short wavelength x-rays and gamma-rays*. Rev. Sci. Instrum. 1947. Vol. 18, No. 9. P. 626–638.

Методи відбиття



Методи проходження

Каналювання заряджених частинок у кристалі з дислокацією та у вигнутому кристалі

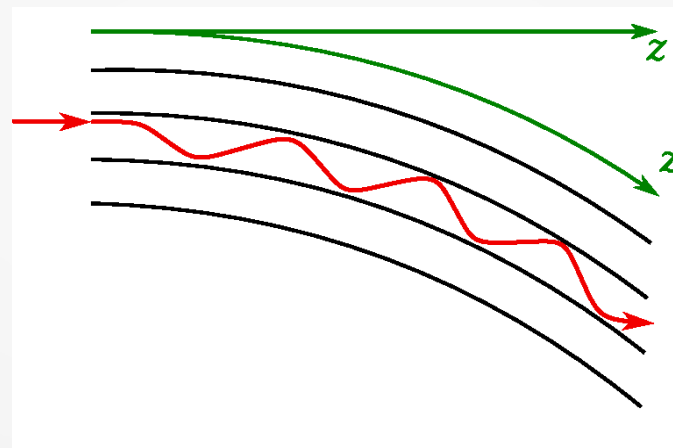
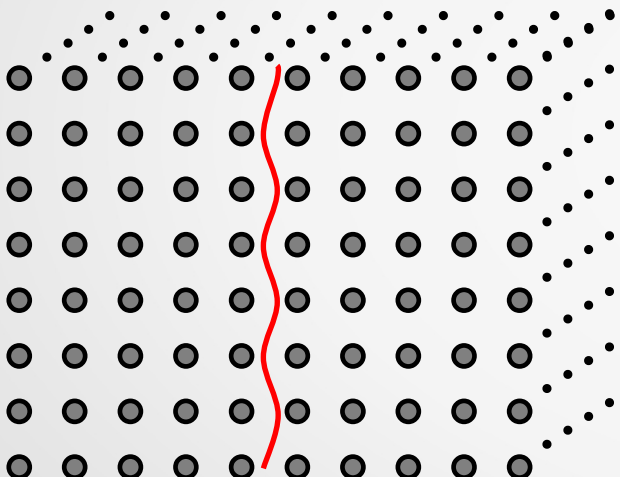


Quéré Y. Dechannelling cylinder of dislocations. Phys. Stat. Solidi B. 1968. Vol. 30, No. 2. P. 713–722.

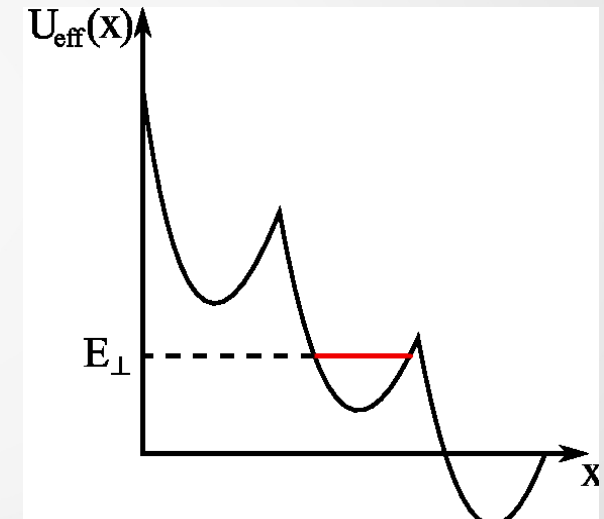
Pathak A. P. Motion of charged particles in curved planar channels: Effects of dislocations. Phys. Rev. B. 1976. Vol. 13, No. 11. P. 4688.

Planar channeling

$$\psi_x < \theta_c, \psi_y \gg \psi_c$$

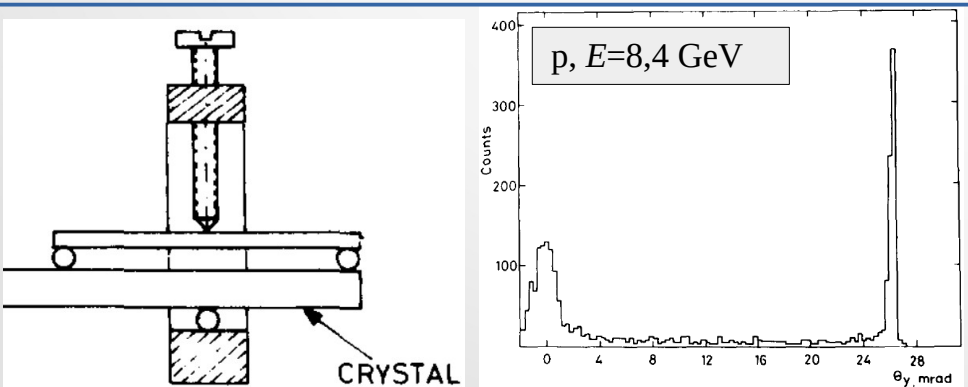
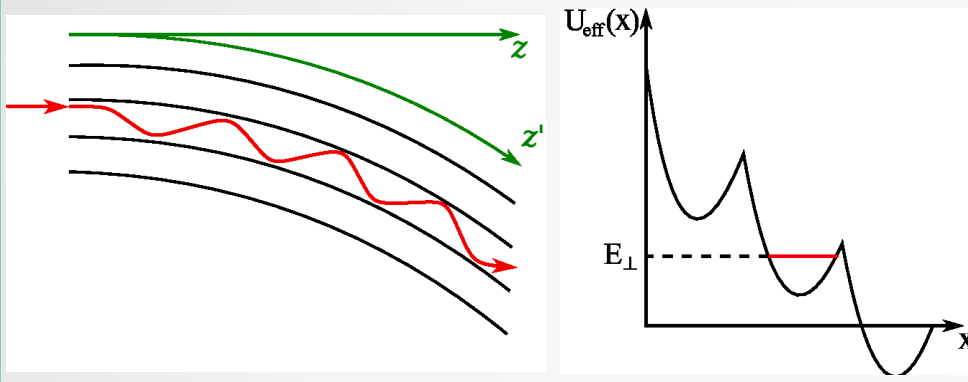


Tsyganov E. N. Fermilab TM-682, TM-684. 1976.

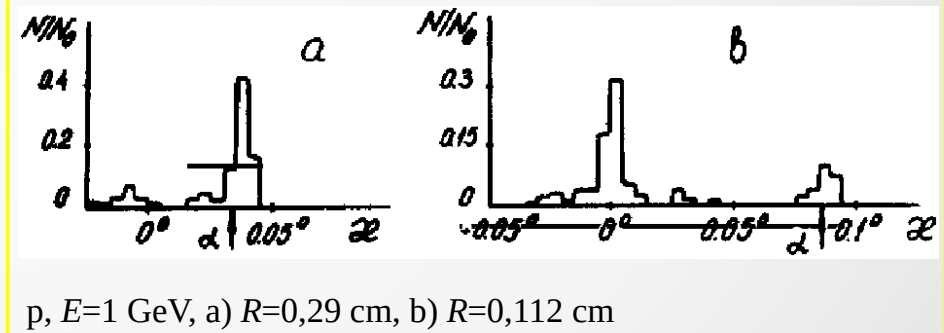


Planar channeling

Tsyganov E. N. Fermilab TM-682, TM-684. 1976.



Tarantin A. M., Tsyganov E. N., Vorobiev S. A. Computer simulation of deflection effects for relativistic charged particles in a curved crystal. *Phys.Lett. A.* 1979. Vol. 72, No. 2. P. 145–146.



p, E=1 GeV, a) $R=0.29$ cm, b) $R=0.112$ cm

Elishev A. F., Filatova N. A., Golovatyuk V. M. et al. (I.A. Grishaev, G.D. Kovalenko, B.I. Shramenko) Steering of charged particle trajectories by a bent crystal. *Phys. Lett. B.* 1979. Vol. 88, No. 3-4. P. 387–391.

Вимірювання магнітного моменту короткоживучих заряджених частинок

Барышевский В. Г. Вращение спина ультрарелятивистских частиц, пролетающих через кристалл. Письма в ЖТФ. 1979. Т. 5, № 3. С. 182–184.

Любошиц В. Л. Поворот спина при отклонении релятивистской заряженной частицы в электрическом поле. Ядерная физика. 1980. Т. 31, № 4. С. 986–992.

$$\frac{d\vec{\zeta}}{d\tau} = \frac{2\mu}{\hbar}\vec{\zeta} \times \vec{H}^* - (\gamma - 1) \left(\vec{l} \times \frac{d\vec{l}}{d\tau} \right) \times \vec{\zeta},$$

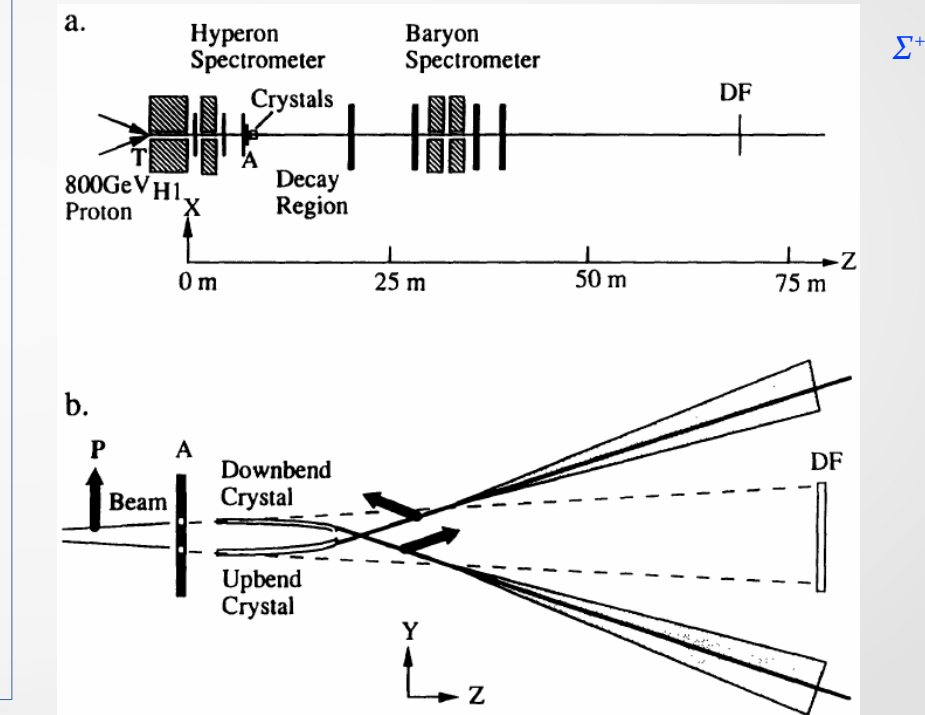
\vec{H}^* напруженість магнітного поля в системі спокою частинки

$\vec{\zeta}$ подвоєне середнє значення оператора спіна частинки

Магнітний момент частинки $\mu = \frac{qg}{2mc}\hbar s$

$$\vec{H}^* = \gamma \left(\vec{H} - \frac{\vec{v}}{c} \vec{l} \times \vec{E} \right) - (\gamma - 1) \vec{l} \left(\vec{l} \cdot \vec{H} \right)$$

$$\theta = \left(\frac{g - 2}{2} \frac{\gamma^2 - 1}{\gamma} + \frac{\gamma - 1}{\gamma} \right) \theta_0$$



Chen D. et al. First observation of magnetic moment precession of channeled particles in bent crystals. Phys. Rev. Lett. 1992. Vol. 69, No. 23. P. 3286–3289. 14

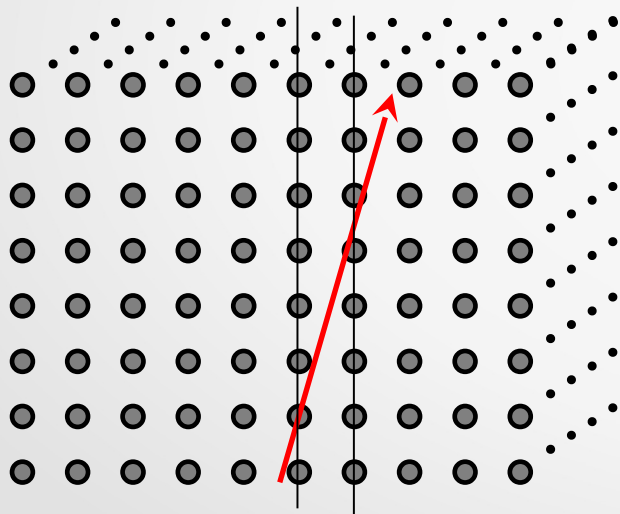
Volume reflection

Taratin A. M., Vorobiev S. A. Phys. Lett. A. 1986. Vol. 115, No. 8. P. 398–400.

Taratin A. M., Vorobiev S. A. Nucl. Instrum. Meth. B. 1987. Vol. 26, No. 4. P. 512–521.

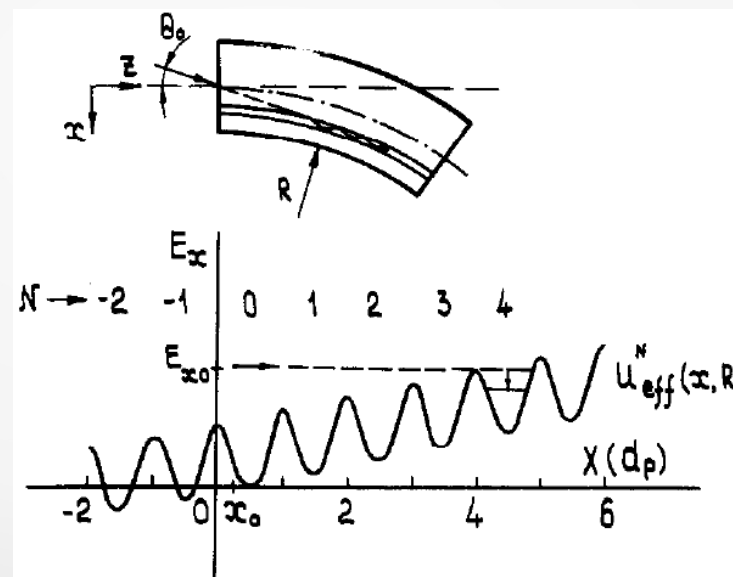
Taratin A. M., Vorobiev S. A. Phys. Lett. A. 1987. Vol. 119, No. 8. P. 425–428.

$$\psi_x > \theta_c, \psi_y \gg \psi_c$$



$$E_x = \frac{pv\theta_x^2}{2} + U_{eff}(x, R)$$

$$U_{eff}(x, R) = U(x) + pv \frac{x}{R}$$

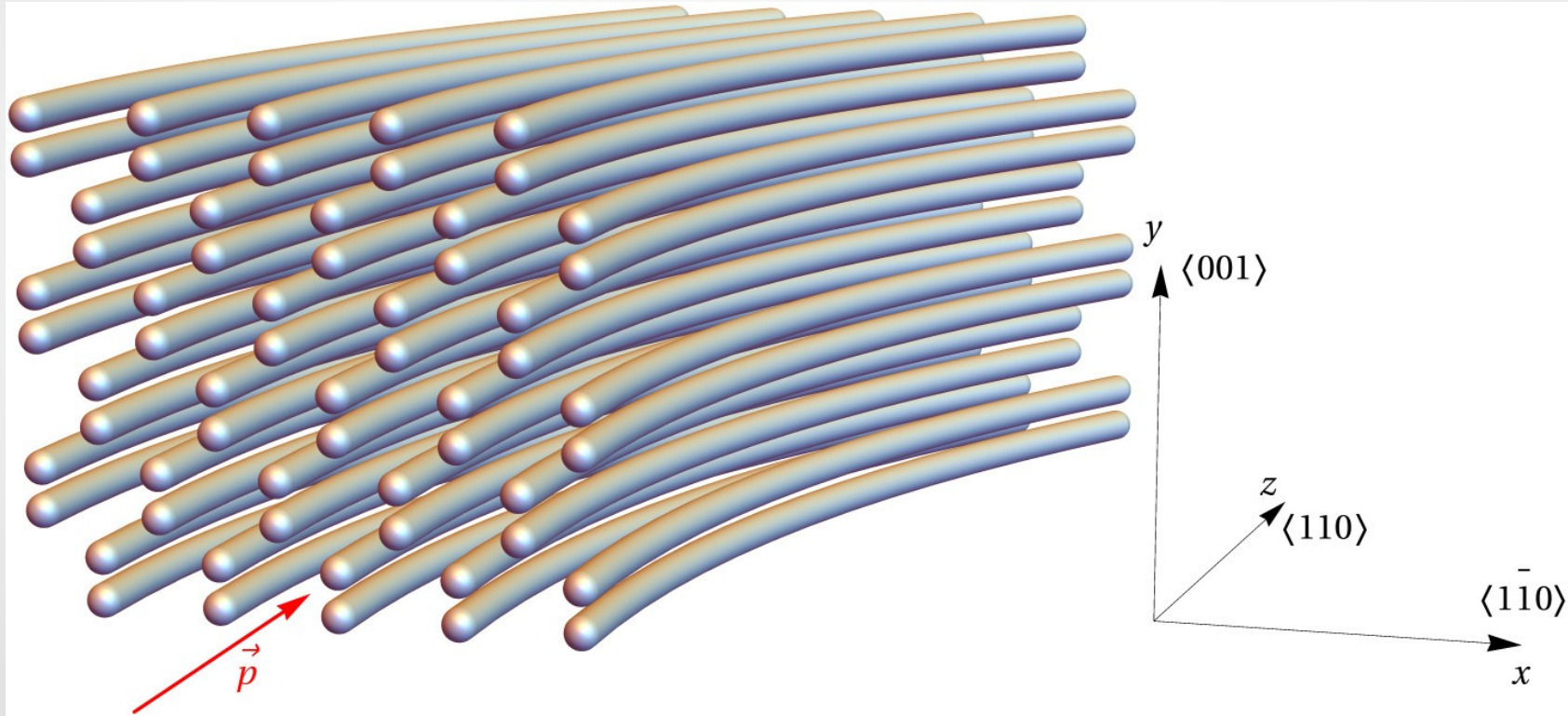


Stochastic deflection

Grinenko A. A., Shul'ga N. F. J. Exp. Theor. Phys. Lett. 1991. Vol. 54. P. 524–528.

Greenenko A. A., Shul'ga N. F. Nucl. Instrum. Meth. B. 1994. Vol. 90, No. 1-4. P. 179–182.

Shul'ga N. F., Greenenko A. A. Phys. Lett. B. 1995. Vol. 353, No. 2. P. 373–377.

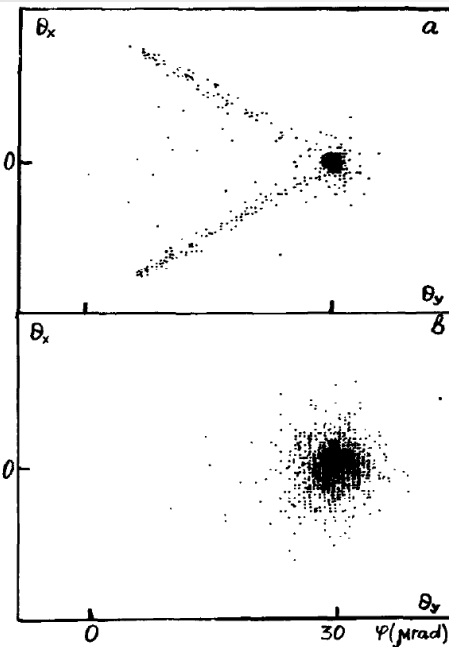


Stochastic deflection

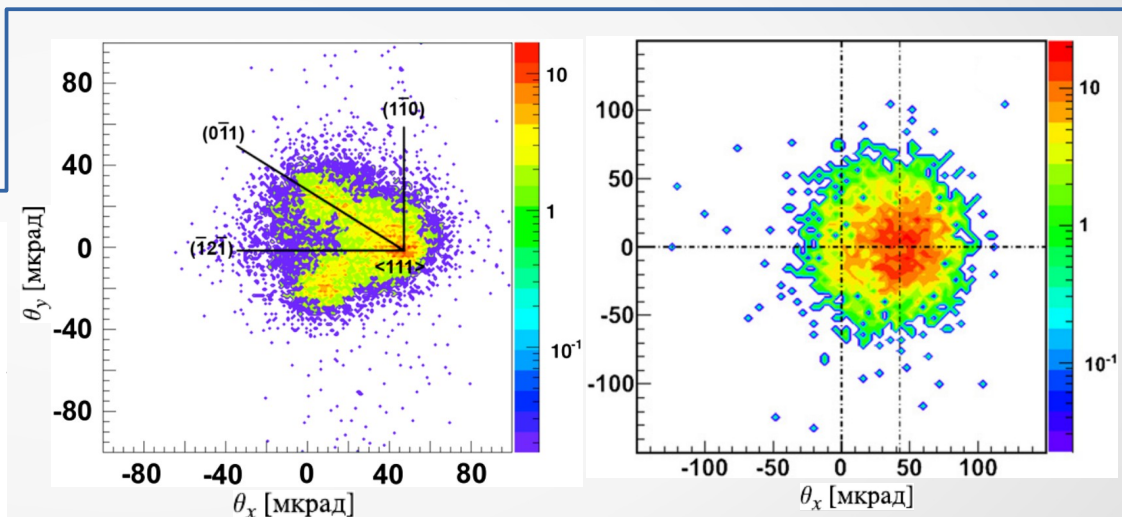
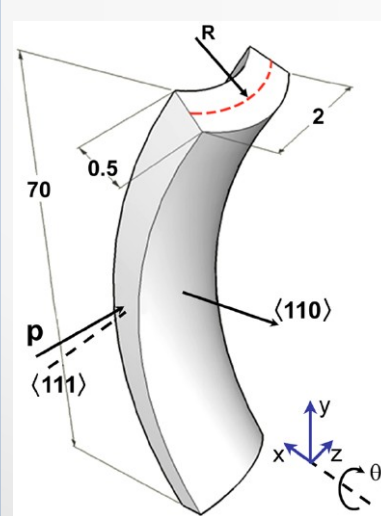
Grinenko A. A., Shul'ga N. F. J. Exp. Theor. Phys. Lett. 1991. Vol. 54. P. 524–528.

Greenenko A. A., Shul'ga N. F. Nucl. Instrum. Meth. B. 1994. Vol. 90, No. 1-4. P. 179–182.

Shul'ga N. F., Greenenko A. A. Phys. Lett. B. 1995. Vol. 353, No. 2. P. 373–377.



$$\langle \psi^2 \rangle = \frac{lL}{R^2} \leq \psi_c^2$$



Scandale W., Vomiero A., Baricordi S. et al. High-efficiency deflection of high-energy protons through axial channeling in a bent crystal. Phys. Rev. Lett. 2008. Vol. 101, No. 16. P. 164801.

Scandale W., Vomiero A., Bagli E. et al. High-efficiency deflection of high-energy negative particles through axial channeling in a bent crystal. Phys. Lett. B. 2009. Vol. 680, No. 4. P. 301–304.

Crystal Bending

Marco Romagnoni et al. Bent Crystal Design and Characterization for High-Energy Physics Experiments. Crystals 2022, 12, 1263. <https://doi.org/10.3390/crust12091263>

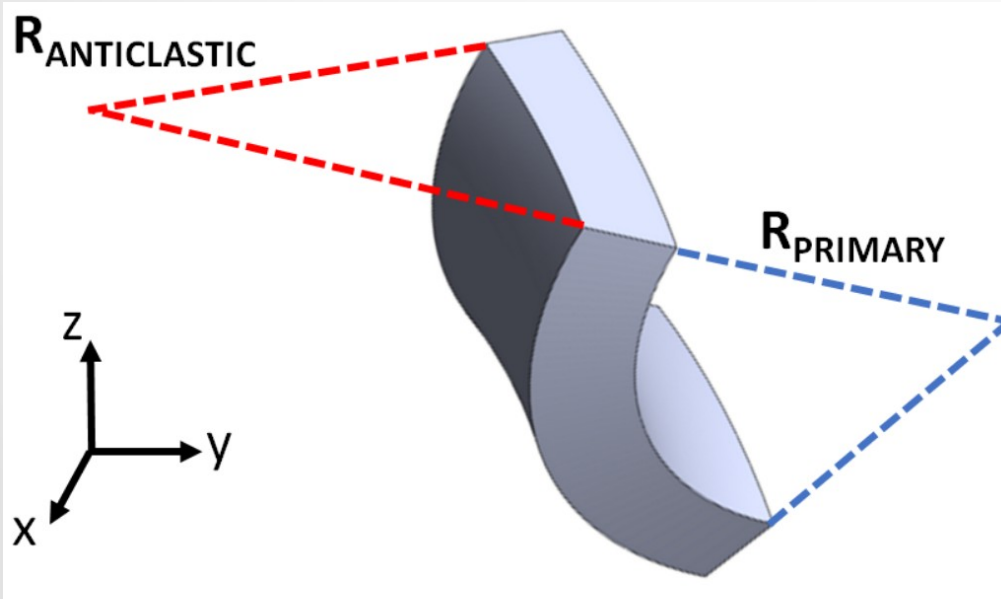


Figure 8. sketch of anticlastic bending state.

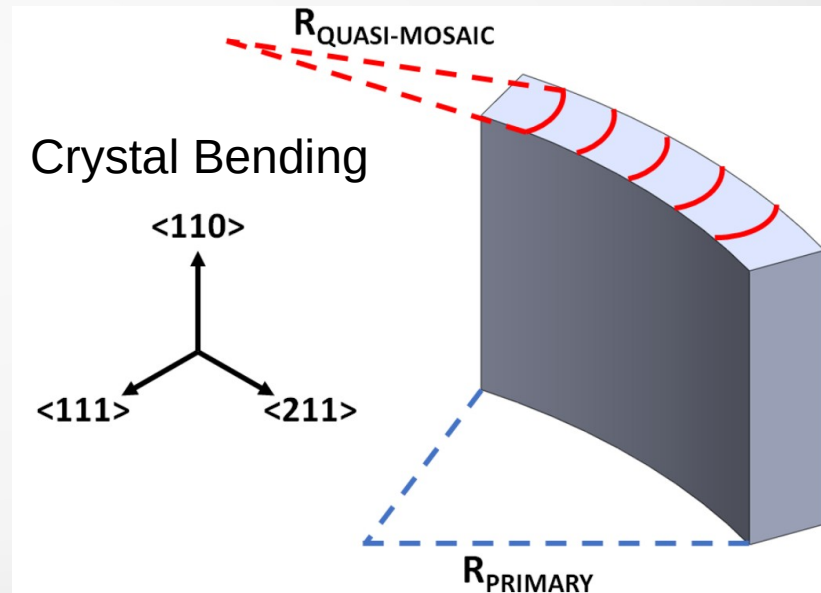
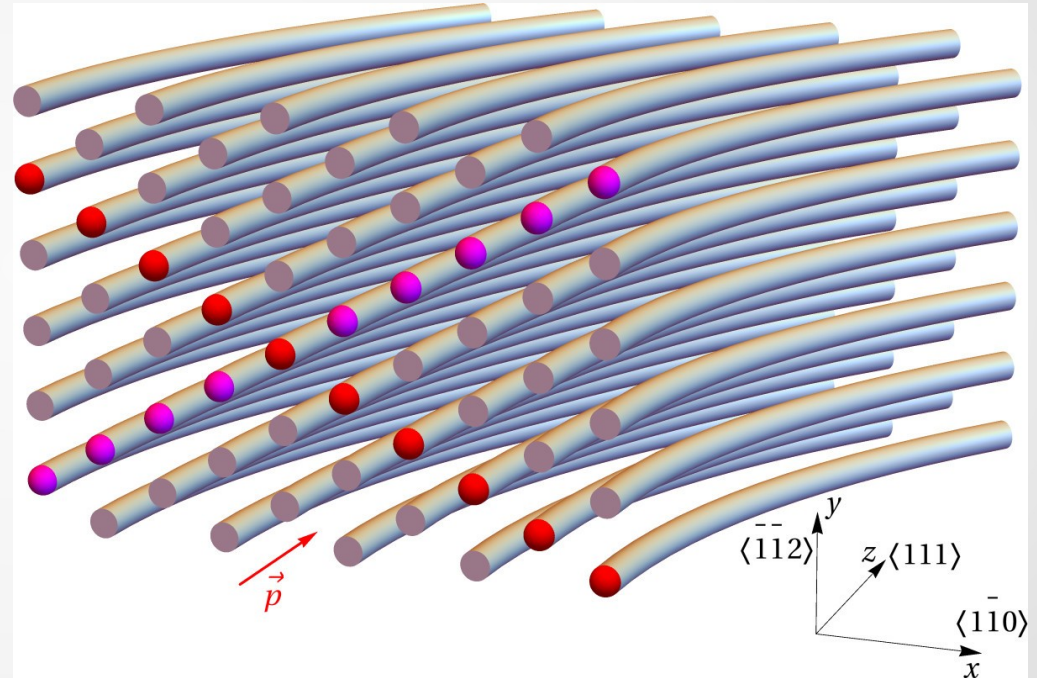
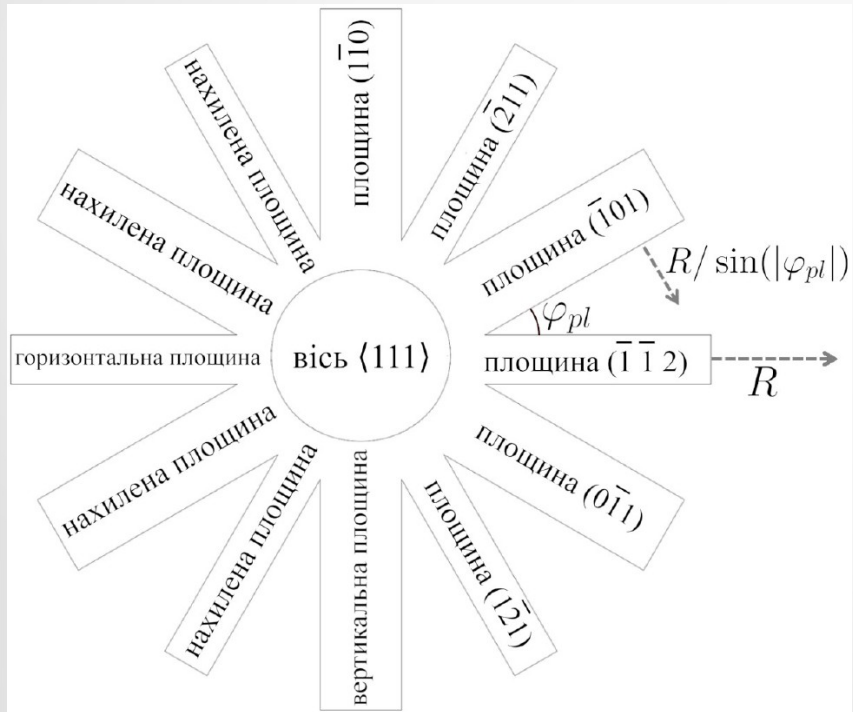


Figure 9. sketch of quasi-mosaic bending state.

Stochastic deflection

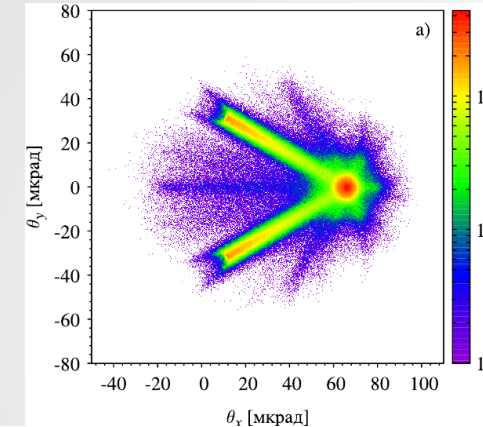
$$\alpha_{st} = \frac{2R\psi_c^2}{l_0}$$

$$R_{cr} = \frac{E \sin |\varphi_{pl}|}{\max \left(\left| \frac{\partial U_{pl}(\zeta)}{\partial \zeta} \right| \right)}$$

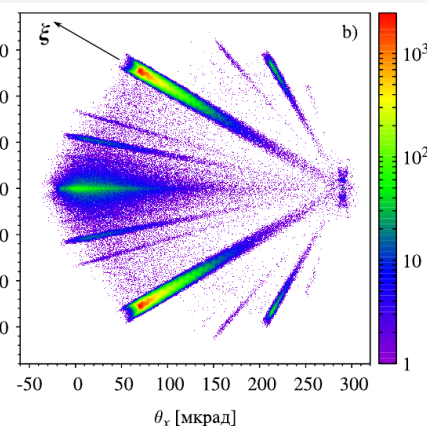


Changing the shape of the beam

$R=30,3\text{ m}$



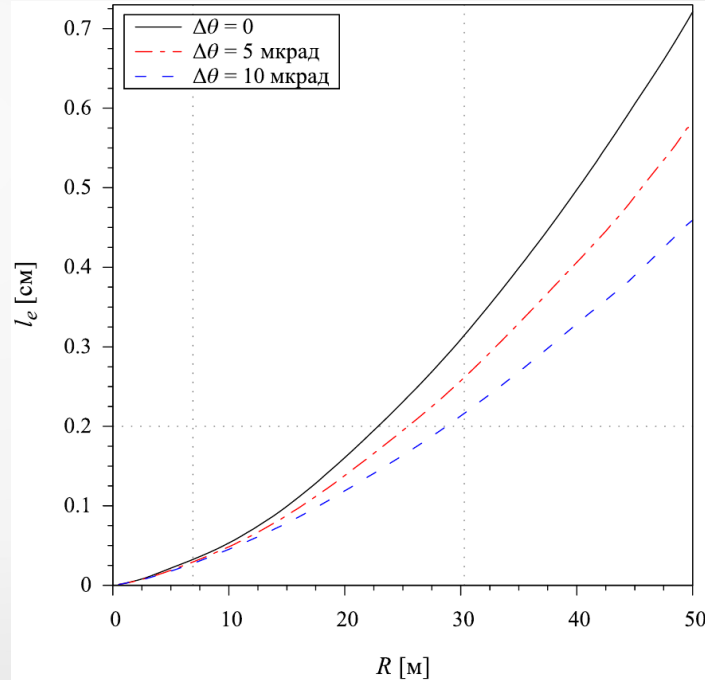
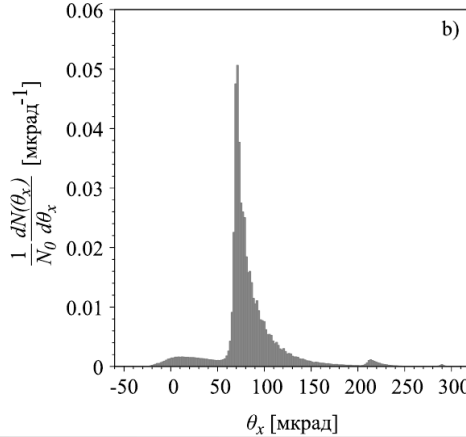
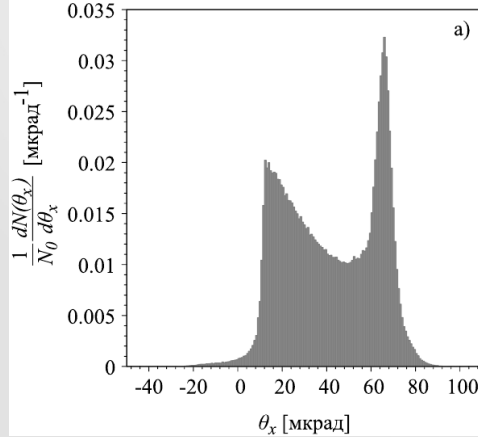
$R=6,9\text{ m}$



$p, E=400\text{ GeV}, \text{Si } <111>, L=2\text{ mm}$

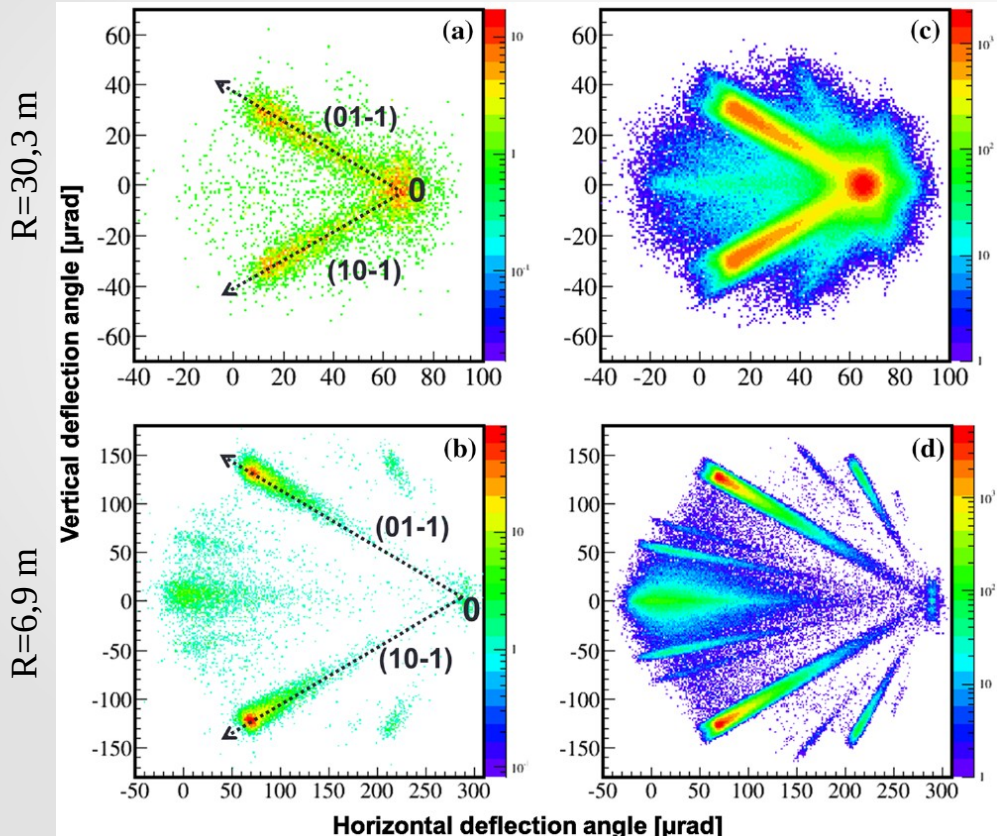
$$|\varphi_{pl}| = \pi/6 \rightarrow R_{cr} \approx 35\text{ cm}$$

$$\frac{dN}{dl} = -CN \rightarrow N_{pl}(l) = N_0 \left(1 - e^{-l/l_e}\right)$$

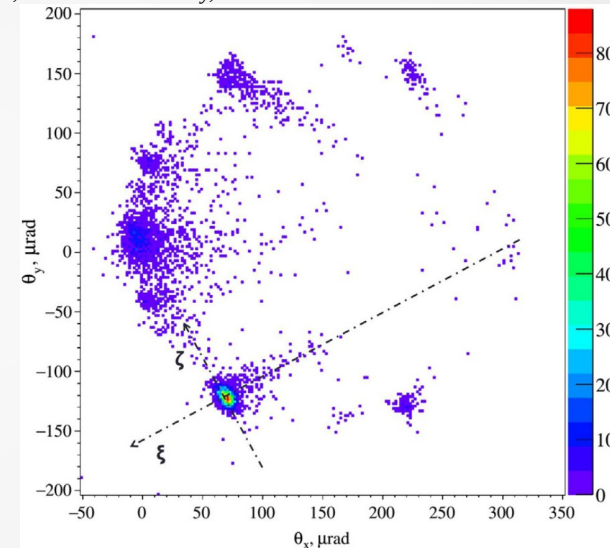


Changing the shape of the beam

$p, E=400 \text{ GeV}, \text{Si } <111>, L=2 \text{ mm}$



$p, E=400 \text{ GeV}, \text{Si } <111>, L=2 \text{ mm}, R=6.9 \text{ m},$
 $\theta_{x,in}=-8 \mu\text{rad}, \theta_{y,in}=-4 \mu\text{rad}$

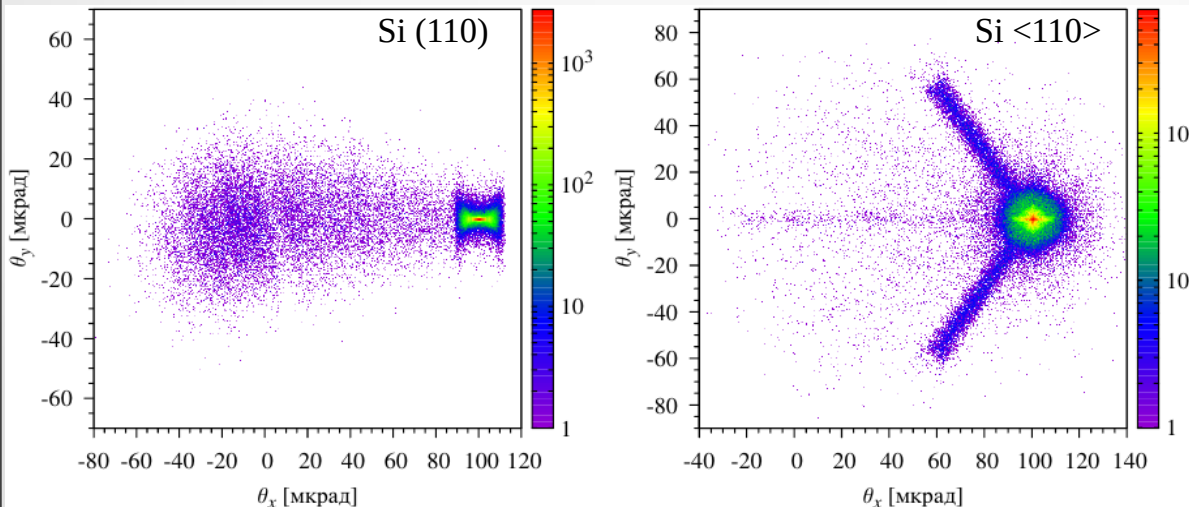
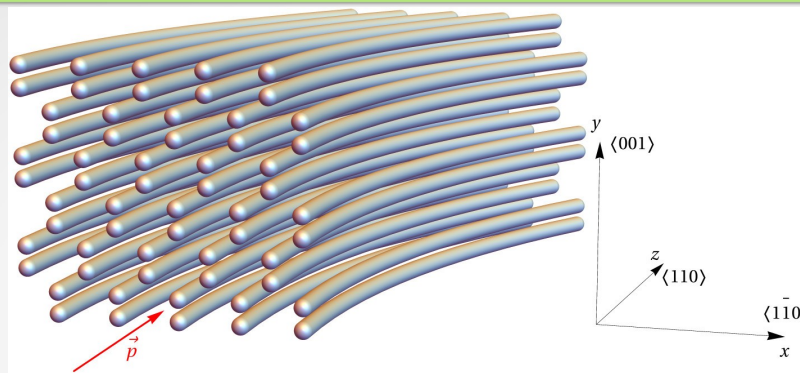


Bandiera L., Mazzolari A., Bagli E. et al. (Kirillin I. V.). Relaxation of axially confined 400 GeV/c protons to planar channeling in a bent crystal. *Eur. Phys. J. C.* 2016. Vol. 76. P. 80 (1–6).

Bandiera L., Kirillin I. V., Bagli E. et al. Splitting of a high-energy positively-charged particle beam with a bent crystal. *Nucl. Instr. Meth. Phys. Res. B*. 2017. Vol. 402. P. 296–299.

Probability of close collisions

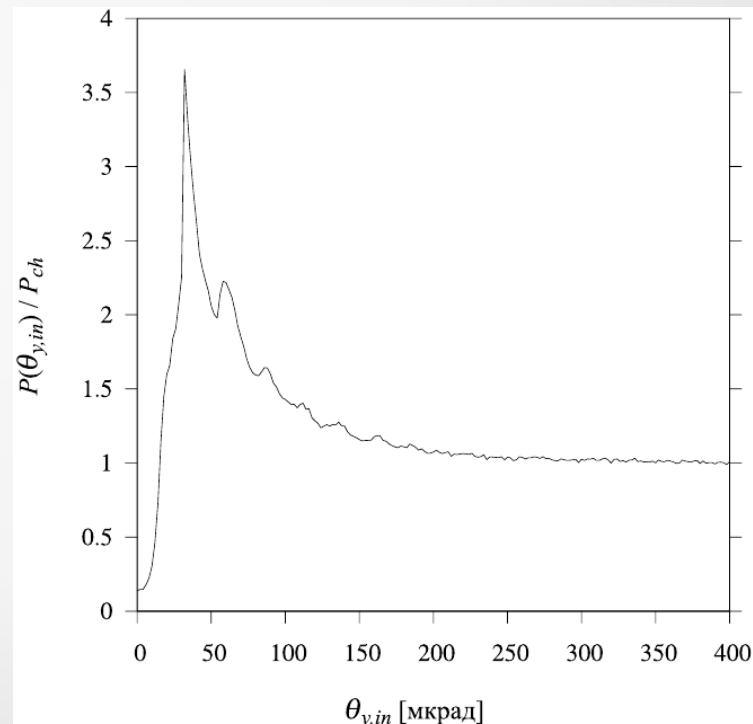
$p, E=270 \text{ GeV}$,
 $\text{Si } <110>, (110)$,
 $L = 5 \text{ mm}$,
 $R = 5 \text{ m}$



Chesnokov Yu.A., Kirillin I.V., Scandale W. et al. Phys. Lett. B. 2014. Vol. 731. P. 118–121.

$$w_a = \frac{4\pi r_T^2}{a_x a_y} = 4\sqrt{2}\pi r_T^2/a^2 \approx 3.39 * 10^{-3}$$

$$w_p = \frac{4r_T}{a_x} = 4\sqrt{2}r_T/a \approx 78.12 * 10^{-3}$$



Probability of close collisions

Scandale W., Arduini G., Butcher M. et al. Phys. Lett. B. 2016. Vol. 760. P. 826–831.

Scandale W., Andrisani F., Arduini G. et al. Eur. Phys. J. C. 2018. Vol. 78, No. 6. P. 505.

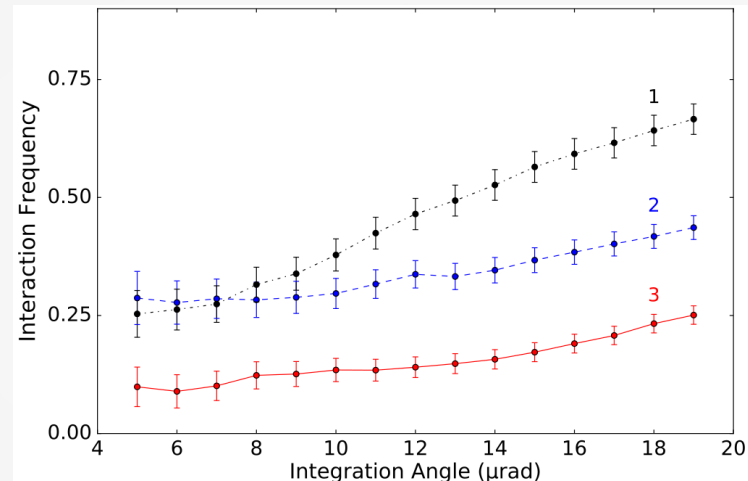
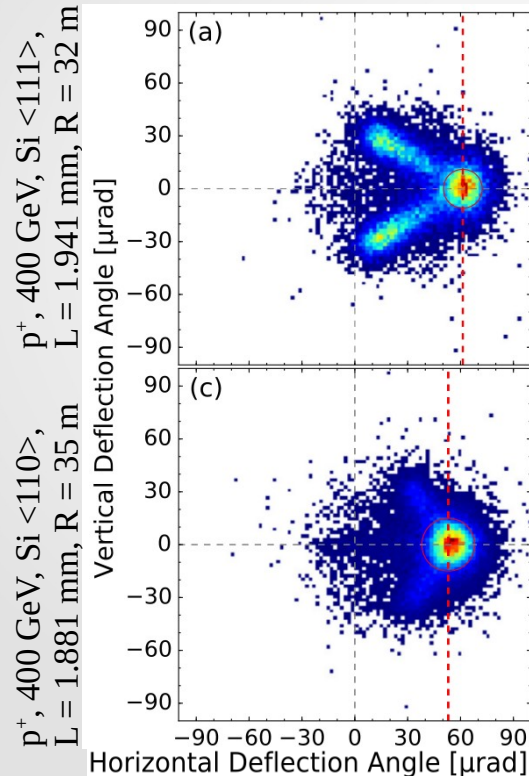
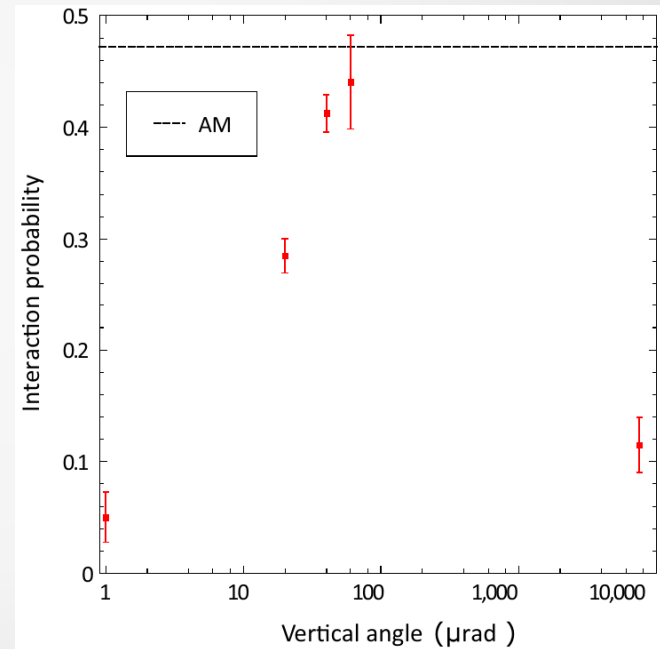
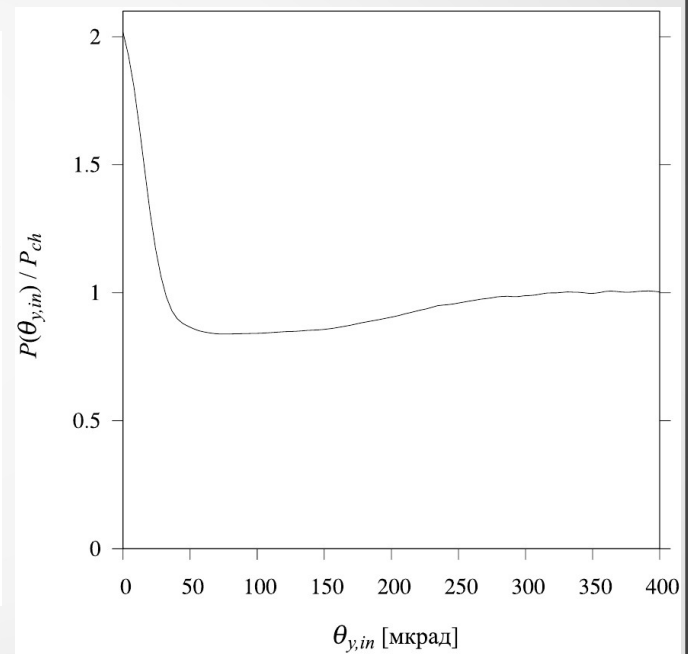
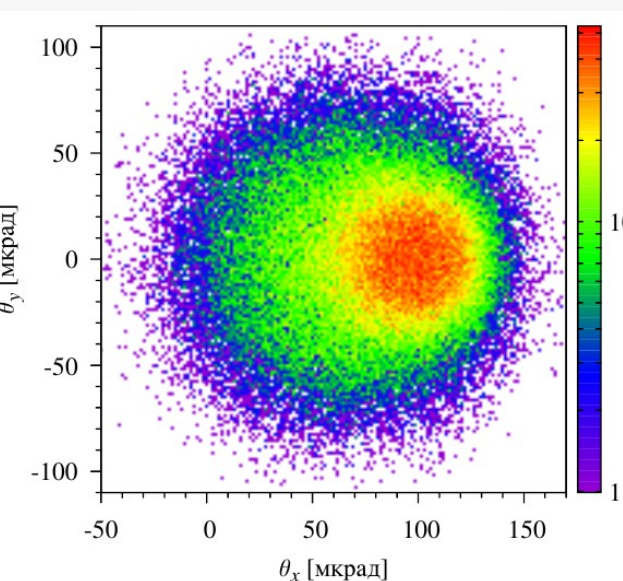
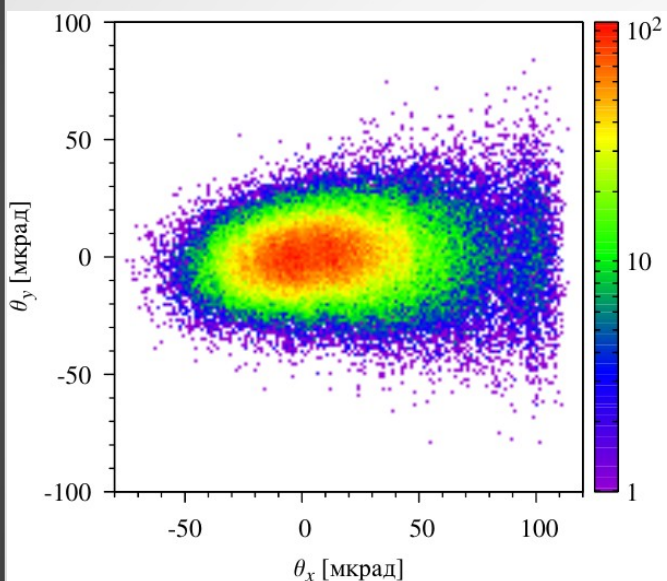


Fig. 5. Measured inelastic nuclear interaction (INI) frequency of 400 GeV/c protons interacting with the $\langle 111 \rangle$ and $\langle 110 \rangle$ crystals as a function of the angular region around the $\langle 110 \rangle$ planar channeling (black dash-dotted line, 1), the $\langle 111 \rangle$ axial channeling (blue dashed line, 2) and $\langle 110 \rangle$ (red continuous line, 3) orientations. The values are normalized to the INI frequencies for the amorphous crystal orientation. (For interpretation of the references to color in this figure legend, the reader is referred to the web version of this article.)



Probability of close collisions

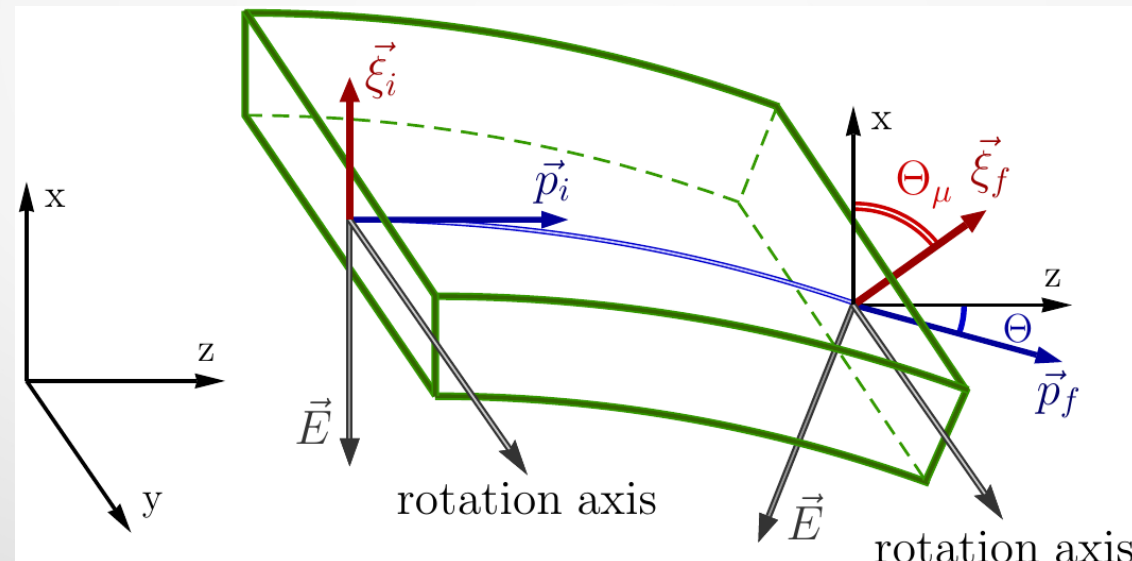
π^- , $E = 270 \text{ ГэВ}$, Si <110>, $L = 5 \text{ mm}$, $R = 5 \text{ м}$



Feasibility of measuring the magnetic dipole moments of the charm baryons at the LHC using bent crystals

Fomin A.S., Korchin A.Yu., Stocchi A. et al. (S.P. Fomin, I.V. Kirillin, N.F. Shul'ga) J. High Energy Phys. 2017. Vol. 2017. № 8. P. 120 (1–26).

$$\Theta_\mu = \gamma \left(\frac{g}{2} - 1 - \frac{g}{2\gamma^2} + \frac{1}{\gamma} \right) \Theta \approx \gamma \left(\frac{g}{2} - 1 \right) \Theta \quad (\text{V.G. Baryshevsky, 1979; V.L. Lyuboshits, 1980})$$



Optimal radius of curvature (stochastic deflection)

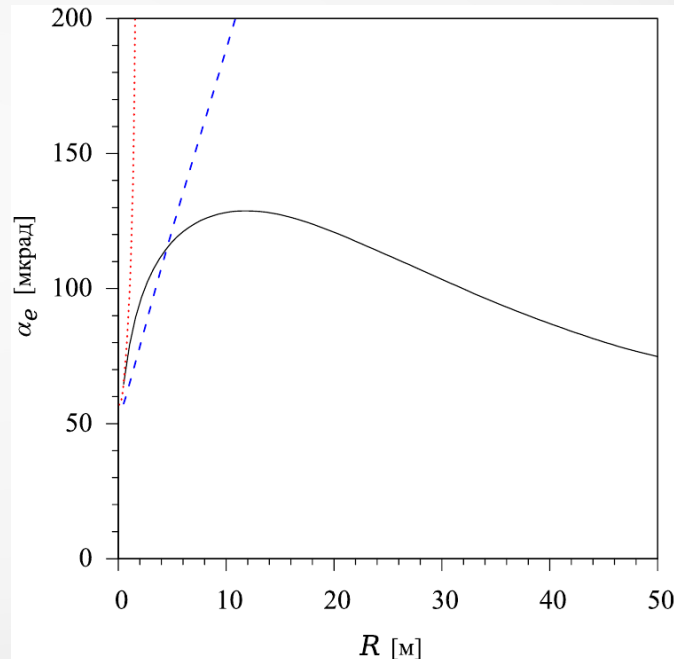
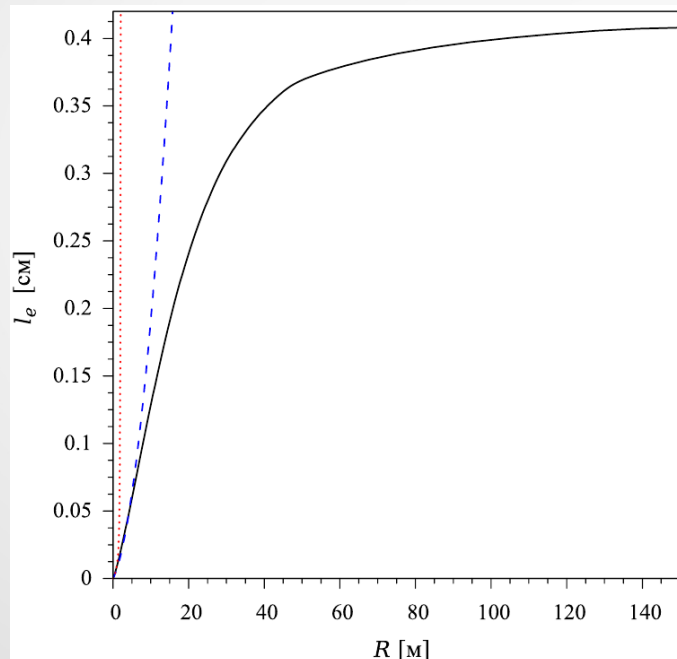
$$\langle \psi^2 \rangle = \frac{lL}{R^2} \leq \psi_c^2$$

$$\overline{\Psi_{inc}^2} = \xi L$$

$$L_{st} = \frac{\psi_m^2}{l/R^2 + \xi}$$

$$\alpha_{st} = \frac{L_{st}}{R} = \frac{\psi_m^2}{l/R + \xi R}$$

π^- , E=150 GeV, Si <110>

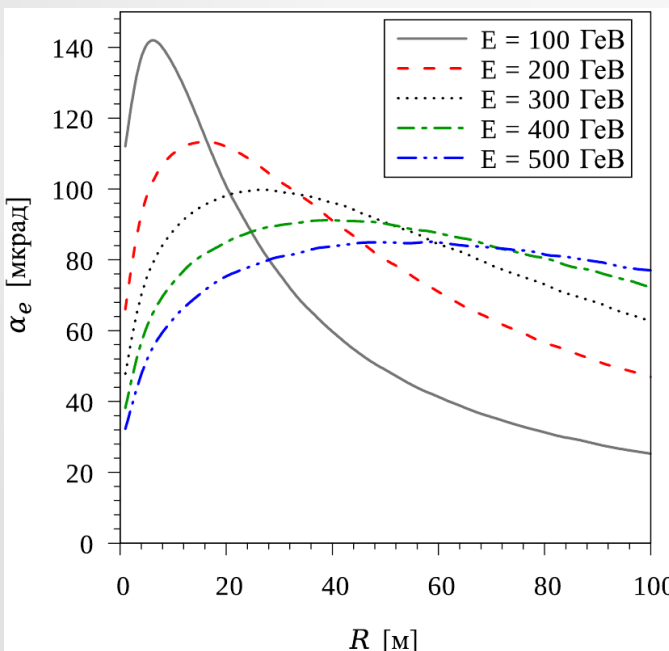


Optimal radius of curvature (stochastic deflection)

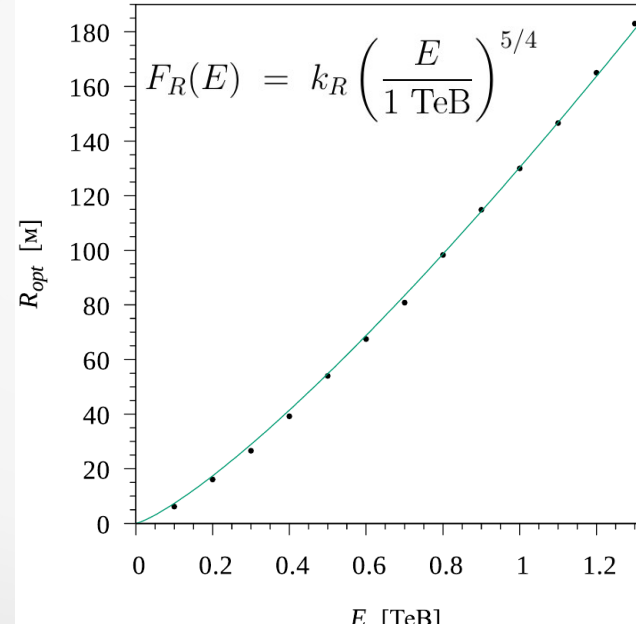
$$\overline{\psi_{inc}^2} = \zeta L/E^2 \rightarrow \alpha_{st} = \frac{\psi_m^2}{l/R + \zeta R/E^2} \rightarrow R_{opt} = E\sqrt{l/\zeta}$$

$$l \approx \frac{1}{4nda} \sqrt{\frac{E}{U_0}} \rightarrow R_{opt} \propto E^{5/4}$$

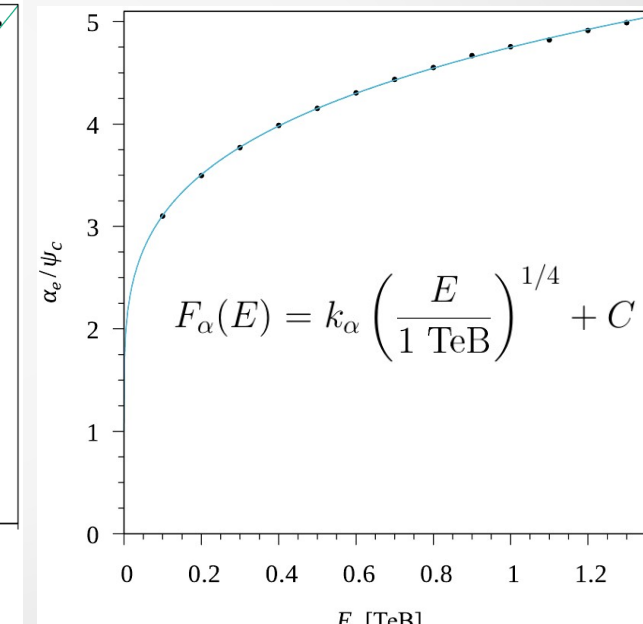
π^- , Si <110>



$$\psi_m \approx 1,5\psi_c \propto E^{-1/2} \rightarrow \max(\alpha_{st}) = \frac{\psi_m^2}{l/R_{opt} + \zeta R_{opt}/E^2} \propto E^{-1/4}$$



$$k_R \approx 130 \text{ m}$$



$$k_\alpha \approx 3,75 \text{ i } C \approx 1 \quad 27$$

Optimal radius of curvature (planar channeling)

$$\frac{d^2x}{dt^2} = -\frac{c^2}{E} \frac{dU_{\text{eff}}(x)}{dx}$$

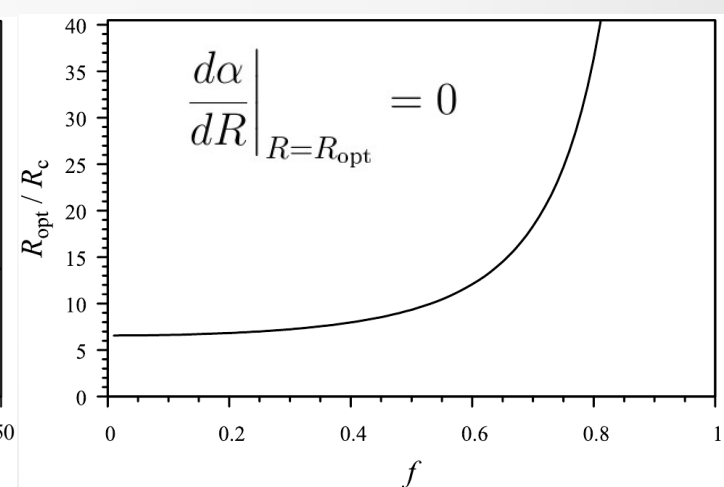
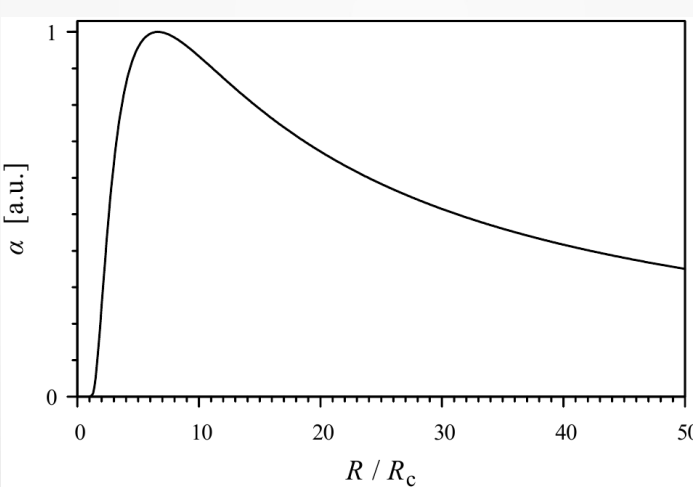
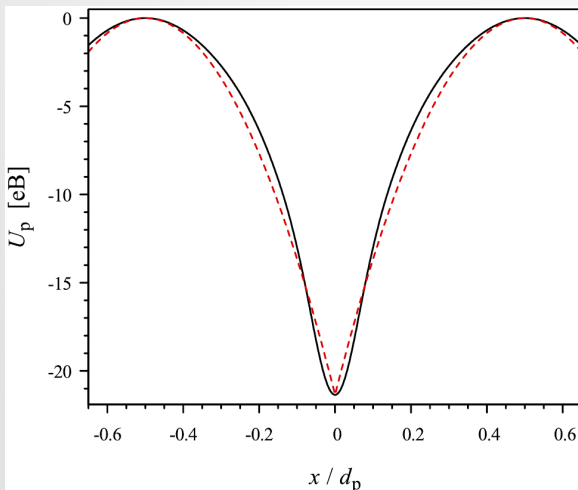
$$U_{\text{eff}}(x) = U_p(x) + Ex/R$$

$$U_p(x) = -\frac{U_0}{d_p^2} ((2x + d_p)^2 H(-x(d_p + x)) + (2x - d_p)^2 H(x(d_p - x)))$$

$$R > R_c \quad \rightarrow$$

$$\frac{x_{\text{pos}} - x_{\text{neg}}}{d_p} = 1 - \sqrt{\frac{R_c}{R}}$$

$$\alpha = \frac{l}{R} = \frac{\theta_c^2}{2\xi_p^2 R \left(\text{erf}^{-1} \left(\frac{f}{1-\sqrt{\frac{R_c}{R}}} \right) \right)^2}$$

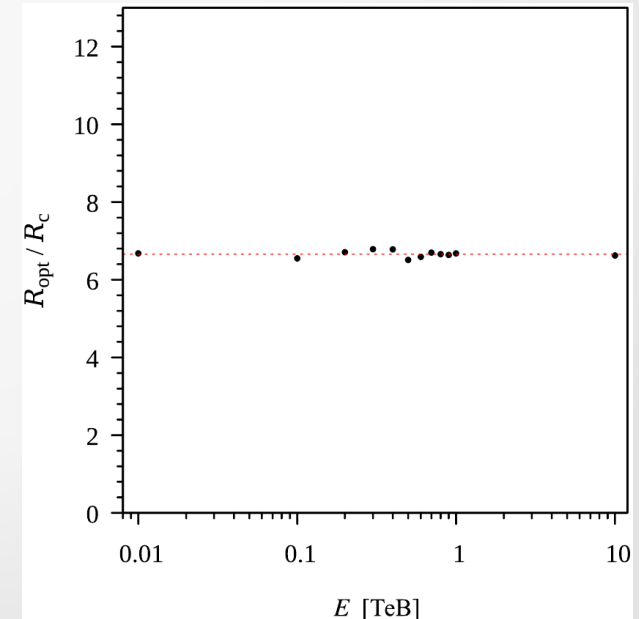
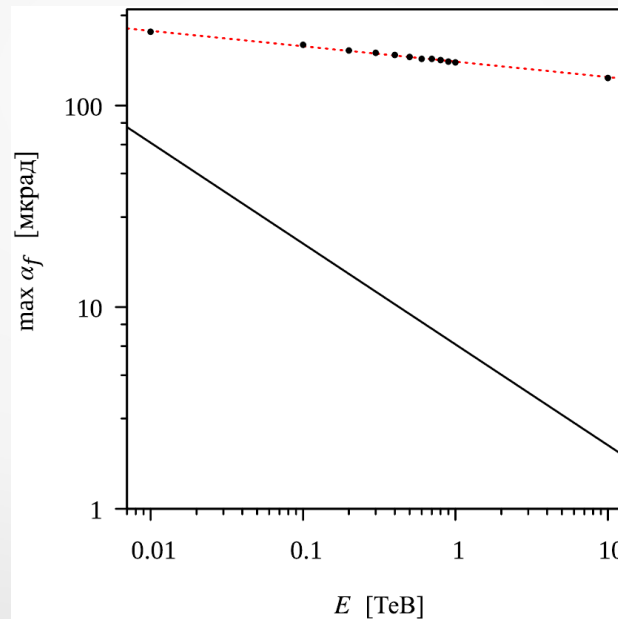
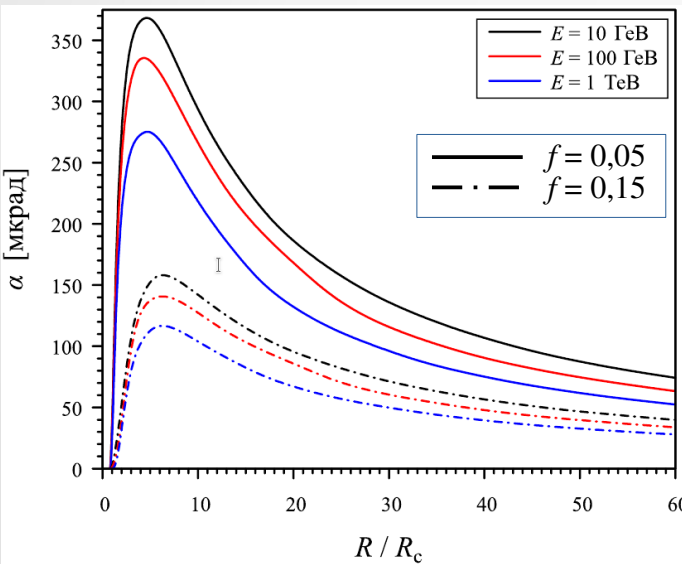


$$\left. \frac{d\alpha}{dR} \right|_{R=R_c} = 0$$

Optimal radius of curvature (planar channeling)

$$U_{\text{str}}(\rho) = -\frac{8\pi^2 \hbar^2}{m_e d} \sum_{k=1}^4 \frac{\alpha_k}{\beta_k + B} e^{-\frac{4\pi^2 \rho^2}{\beta_k + B}} \rightarrow U_{\text{pl}}(x) = -\frac{4\pi^{\frac{3}{2}} \hbar^2}{m_e d d_s} \sum_{k=1}^4 \frac{\alpha_k}{\sqrt{\beta_k + B}} e^{-\frac{4\pi^2 x^2}{\beta_k + B}}$$

$$U_p(x) = \sum_{n=-\infty}^{\infty} U_{\text{pl}}(x - x_n) \rightarrow U_p(x) = -\frac{2\pi \hbar^2}{m_e d d_s d_p} \sum_{k=1}^4 \alpha_k \theta_3 \left(\pi \frac{x}{d_p}, e^{-\frac{\beta_k + B}{4d_p^2}} \right)$$



W. Scandale et al. Observation of channeling for 6500 GeV/c protons in the crystal assisted collimation setup for LHC. Phys. Lett. B 758 (2016) 129

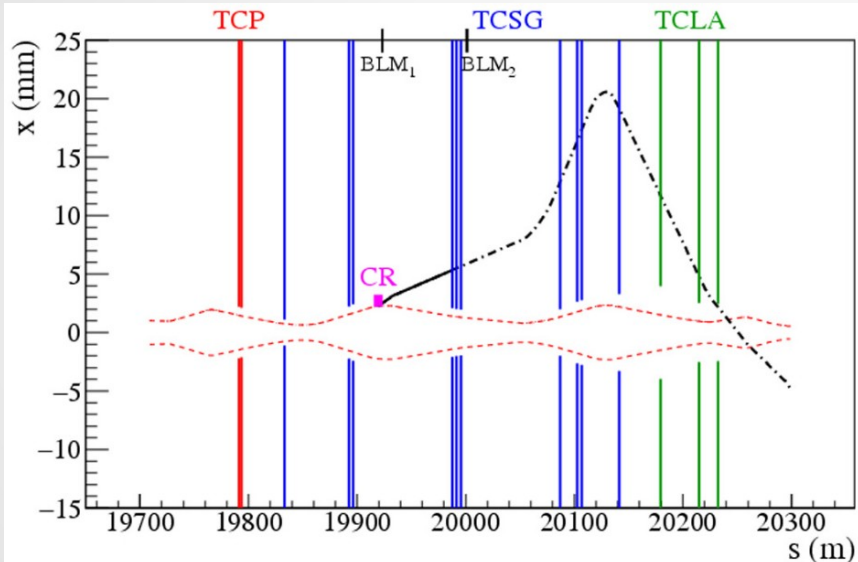


Fig. 1. (Color online.) The horizontal projection of the trajectory of a halo particle deflected by the crystal due to channeling at the bend angle $\alpha = 65 \mu\text{rad}$ (solid line up to the first horizontal TCSG_1 and then by dot-dashed line to show the trajectory propagation in the case without the collimators): (a) for the beam injection with

TCP -- primary collimators
TCSG -- secondary collimators

TCLA -- shower-absorber collimators
made from a tungsten heavy alloy

Marco D'Andrea et al. Characterization of bent crystals for beam collimation with 6.8 TeV proton beams at the LHC. NIM A 1060 (2024) 169062

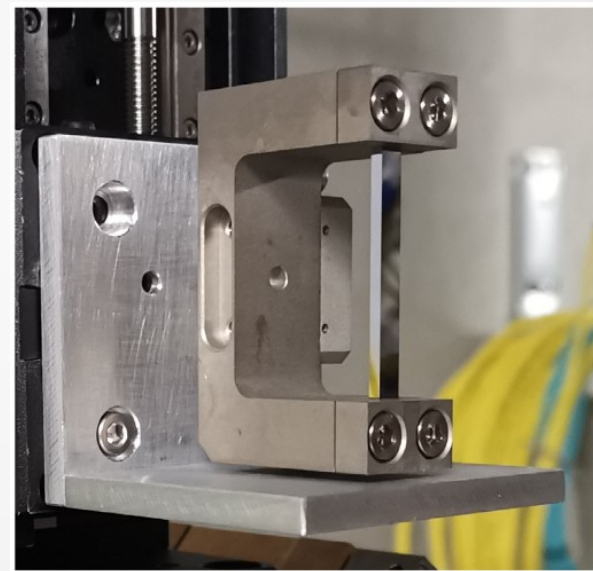
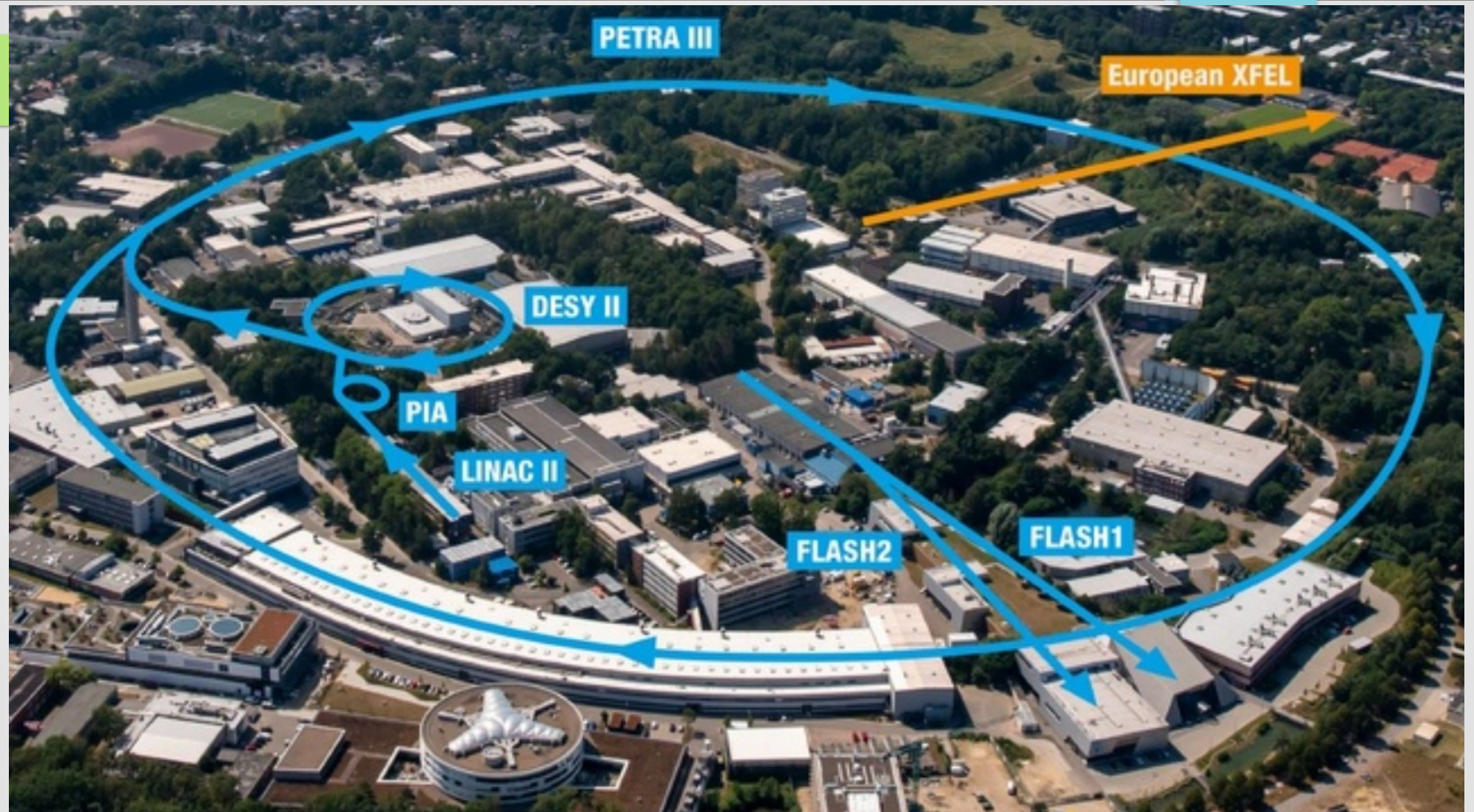
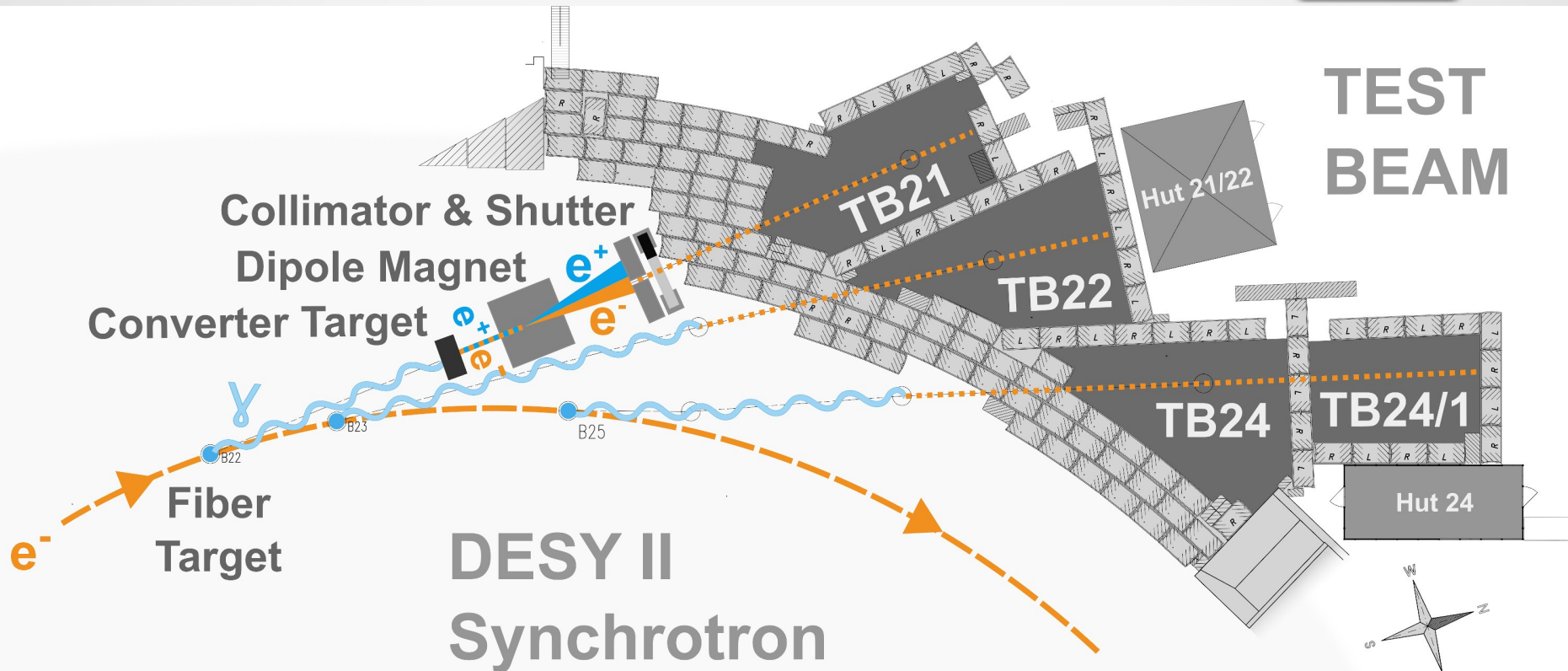


Fig. 2. Picture of a Si crystal clamped by its metal holder.

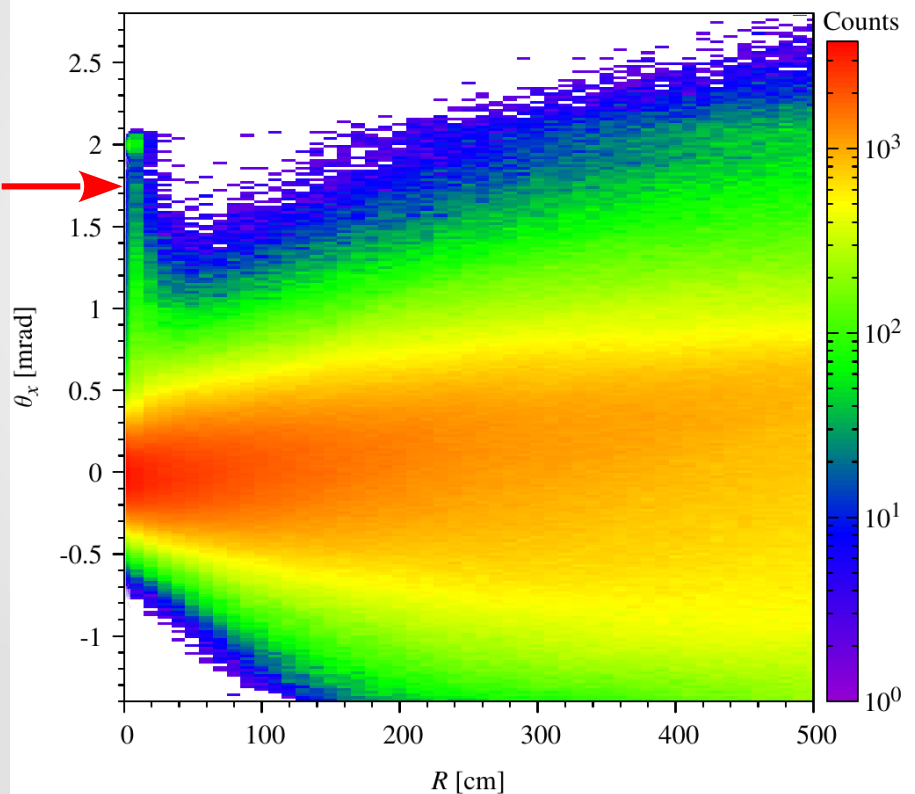


Generation of the DESY Test Beams

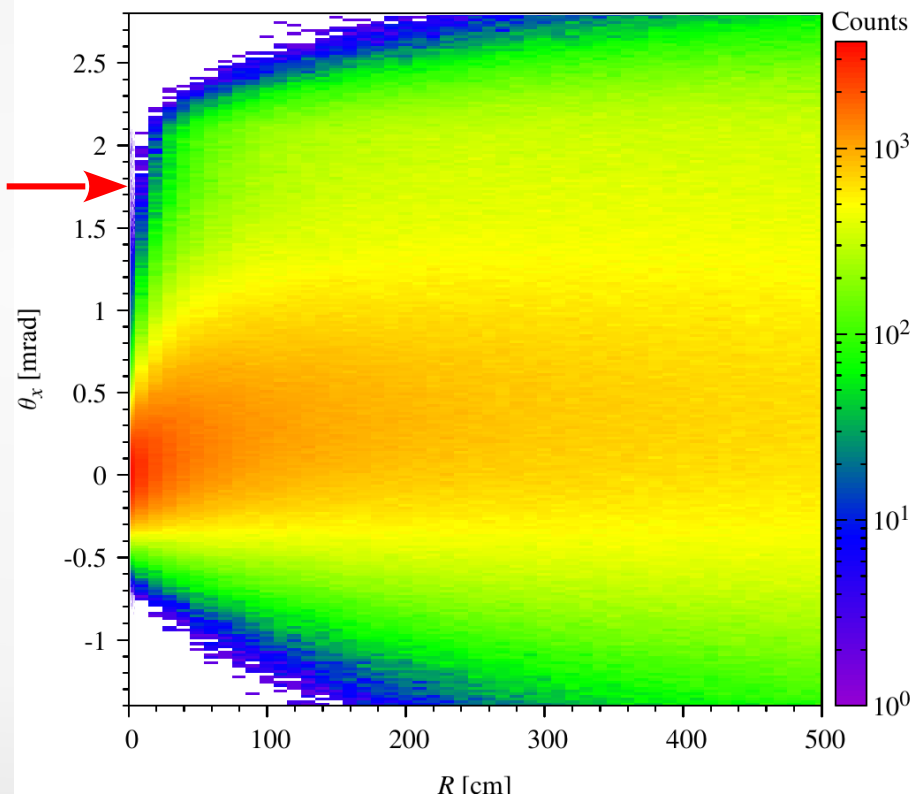


- Dependence of deflection angle on R ($\alpha = 2$ mrad)

(111) plane



(110) axis





Thank you for your attention!